

Article

Variability of Near-Surface Aerosol Composition in Moscow in 2020–2021: Episodes of Extreme Air Pollution of Different Genesis

Dina Petrovna Gubanova * , Anna Aleksandrovna Vinogradova , Mikhail Alekseevich Iordanskii and Andrey Ivanovich Skorokhod

A.M. Obukhov Institute of Atmospheric Physics, Russian Academy of Sciences, Pyzhyovskiy Pereulok, 3, 109017 Moscow, Russia; anvinograd@yandex.ru (A.A.V.); miordan@mail.ru (M.A.I.); skorokhod@ifaran.ru (A.I.S.)
* Correspondence: gubanova@ifaran.ru or dgubanova@mail.ru

Abstract: During 2020–2021, a comprehensive experiment was conducted to study the composition of near-surface atmospheric aerosol in Moscow. The paper considers the experimental data together with synoptic and meteorological conditions. Attention is focused on six episodes of extremely high aerosol mass concentration values: in March and October 2020, as well in March, April, May and July 2021. In all these cases (and only in them), the average daily mass concentration of PM₁₀ aerosol exceeded the Maximum Permissible Concentration (MPC) value (according to Russian standards, 60 µg/m³). The origin of the aerosol during these periods of extreme pollution is revealed, which is the main result of the work. It was shown that the July episode of 2021 was associated with a local intensive anthropogenic source that arose as a result of the active dismantling and demolition of multistory industrial buildings. The remaining spring and autumn episodes were caused by atmospheric transport of both smoke aerosol from various regions with strong biomass fires and dust aerosol from arid zones of the south of European territory of Russia (ETR) with dust wind storms. The cases of atmospheric pollution transport to Moscow region from the other regions are confirmed with the help of air mass transport trajectories (HYSPLIT 4 model) and MERRA-2 reanalysis data on black carbon and/or dust distribution in the atmosphere over ETR. Differences in the elemental composition of the near-surface aerosol of Moscow air during periods with extremely high aerosol concentrations are analyzed in comparison with each other and with unperturbed conditions for the season.

Keywords: atmosphere; long-range and regional transport; near-surface aerosol; particulate matter (PM₁₀); sources; mass concentration; elemental composition; enrichment factor



Citation: Gubanova, D.P.; Vinogradova, A.A.; Iordanskii, M.A.; Skorokhod, A.I. Variability of Near-Surface Aerosol Composition in Moscow in 2020–2021: Episodes of Extreme Air Pollution of Different Genesis. *Atmosphere* **2022**, *13*, 574. <https://doi.org/10.3390/atmos13040574>

Academic Editor: Liudmila Golobokova

Received: 28 February 2022

Accepted: 31 March 2022

Published: 3 April 2022

Publisher's Note: MDPI stays neutral with regard to jurisdictional claims in published maps and institutional affiliations.



Copyright: © 2022 by the authors. Licensee MDPI, Basel, Switzerland. This article is an open access article distributed under the terms and conditions of the Creative Commons Attribution (CC BY) license (<https://creativecommons.org/licenses/by/4.0/>).

1. Introduction

The study of composition and quality control of the air of cities has been one of the most pressing problems for all countries and regions in recent years [1]. Aerosol—the most active and dynamic component of the atmosphere—serves as an indicator of ecosystem state and also indicates possible sources of pollution. The main sources of natural aerosols in cities and industrial areas are the soil and, to a lesser extent, sources of bio-aerosols. Primary anthropogenic aerosols are released into the atmosphere by industrial enterprises, heat power industry and transport. Secondary aerosols, which are mostly the particles of a fine (submicron) fraction, are formed during microphysical and photochemical processes involving water vapor, organic compounds and various precursor gases [2].

The mixing of anthropogenic and natural emissions in near-surface air creates a heterogeneous field of pollutants, which changes rapidly due to the mobility of air masses, the influence of meteorological conditions and active chemistry of gases and aerosols in urban conditions. In addition, large cities are characterized by specific features: heterogeneity

of urban development, the presence of recreational landscapes, complex natural and anthropogenic orography, a special wind regime, the impact of “heat island”, the different types of local anthropogenic sources, etc. All these aspects influence strongly in spatial and temporal variability of urban aerosols (their size distribution and chemical composition) and create difficulties for studying atmospheric composition in metropolis.

Currently, the attention of the scientific community is focused on so called climate significant atmospheric components, including, in addition to greenhouse gases and ozone, such aerosol components as dust and black carbon (BC) [3,4]. These components change optical properties and radiation parameters of the atmosphere. Further, in high concentrations, they affect negatively the health of urban people [2,5–12]. Under stable conditions, local anthropogenic and natural sources should create more or less stable average level of aerosol atmospheric pollution in the city (“background”, different for each season) less than Maximum Permissible Concentration (MPC) value for residential territories. However, dust and smoke aerosol emissions can be transported in the atmosphere up to the distances of several thousand kilometers [9–15] and can make a significant contribution to urban atmosphere pollution [16]. In such cases, in city air, an extremely high aerosol pollution is formed, the various components of which are of natural and/or anthropogenic origin, as well as having local and/or remote sources.

Elevated or extremely high values (in comparison with the average characteristics and MPC values) of mass concentrations of BC and PM₁₀ and PM_{2.5} aerosols are occasionally recorded (within a few days) in the near-surface air of Moscow [17–27]. In most cases, this is due to the atmospheric transport of air masses containing pollutants from natural fires or anthropogenic biomass burning on neighboring or more remote territories, as well as from dust storms in remote semiarid areas of the south of European territory of Russia (ETR). The extremely hot and dry summer of 2010 can serve as a striking example of such pollution of the atmosphere in the region of Moscow [23,28,29]. At that time, numerous forest and peat fires broke out in the center of the ETR, and a steady (for almost a month) anticyclone accumulated and mixed air impurities over almost the entire territory of the ETR except for the northernmost regions. Another example of long-range atmospheric transport of fire aerosols to Moscow was connected with the eastern air mass transport from the wildfires in the southern regions of Western Siberia to the west, up to Moscow and further to Europe in 2016 [22,30].

It should be noted that in recent years, scientists around the world have paid increased attention to studying the sources and properties of fire aerosols, conditions and processes of their transport, as well as the assessment of their impact on the composition of the atmosphere, urban ecosystems and the climate of the Earth (for example, [7,8,13–23,30–35]). In particular, various markers of combustion products [31,32], the contributions of various sources to carbon-containing aerosols [33], the influence of meteorological conditions on the composition and transport of smoke aerosols [34–39] were studied with the help of numerical modeling, laboratory experiments, satellite and ground-based observations [15,16,31–43].

Another significant climate component of aerosols, dust, has also been studied in detail at present. As is known [12,44,45], the main natural sources of dust aerosol are the arid and semi-arid regions of the globe, the largest of which are located in North Africa, the Arabian Peninsula and the Middle East, and Central and East Asia. A number of published works are devoted to the transatlantic transport of Saharan dust to North and South America [46–50], as well to Europe [51–57]. Assessments of radiation forcing from dust aerosols of various source regions to climate characteristics of the global atmosphere have been carried out [58–64]. A more detailed review of literary sources on this theme is presented in [27].

However, there is practically no work on atmospheric transport of dust from arid and semi-arid regions to the middle latitudes of Eastern Europe and ETR. However, the results of studies (including those considered in this article) show that in the absence of fire impacts (in particular, in the cold season), significant air pollution with dust can be observed at

the latitude of Moscow during atmospheric transport from remote territories [27]. The amplitude of such impacts is comparable to the impact of local sources associated, for example, with active traffic, intensive work on the destruction/construction of buildings, repair and reconstruction of courtyards and streets, etc. [65]. Estimates [66–68] of the probabilities of long-range atmospheric transport of natural silicates (the basis of dust aerosol in Moscow and its suburbs) from various source regions to Moscow region showed that the most likely sources are situated in the Aral Sea region and arid areas of the Russian coast of the Caspian Sea (Kalmykia and Astrakhan region). The average duration of aerosol transportation from these regions to Moscow is 3–5 days. The impacts of such powerful sources of dust aerosol as the deserts of Northern Africa, the Middle East and the South of Central Asia are much weaker due to their remoteness and the rarity of air mass transport from them to the Moscow region.

This study examines the results of continuous two-year observations of the near-surface aerosol composition in Moscow. Special attention is paid to episodes of high aerosol concentration (more than MPC value for particles PM_{10}) in the urban air in different seasons of the year. The sources of extreme aerosol pollution of various origins are discussed. The variability of mass concentration and elemental composition of atmospheric aerosol is analyzed during these episodes and in their absence.

2. Materials and Methods

2.1. Object, Place and Means of Observation

Moscow is the largest metropolis in Europe (area > 2.5 million km^2 , population > 12.5 million people), located in the central part of the European Territory of Russia (ETR). It is characterized by all the specific features inherent in the largest cities in Europe. The development of urban infrastructure has trends similar to the development trends of large modern cities. The administrative, business and shopping centers are concentrated in the central part of the city. The main anthropogenic sources of air pollution in the central district of Moscow are transport, thermal power plants, food industry and household services. Enterprises of various industries are located in industrial areas at a distance from the center [69–72].

The observation point is located at A.M. Obukhov Institute of Atmospheric Physics (IAP) RAS (Pyzhyovskiy Pereulok, 3, Moscow, Russia), in a zone of dense administrative and residential development with sealed asphalt-concrete landscapes, at a distance from major highways and railways (Figure 1). The experimental measuring complex is located in a separate standing building (55.74° N; 37.62° E) in the courtyard of the Institute.

The objects of research were the physicochemical characteristics of submicron and micron sized aerosol particles in near-surface layer of the atmosphere: microphysical parameters, elemental composition, morphological structure and mass concentration.

During 2020–2021, a comprehensive seasonal experiment was conducted, including:

- measurement of the distribution of the number of aerosol particles by size (the number distribution) by aerosol spectrometers, in continuous automatic mode with a time resolution of 5 min;
- daily (for 35–40 days in each season) sampling for analytical aerosol filters using an aspiration sampler for gravimetric and elemental analysis of the samples obtained;
- seasonal sampling by a 6-cascade impactor to determine sized distributions of mass concentration and elemental composition of aerosols.

The experimental complex is described in more detail in [26,65].

Explanations to the scheme of Figure 1. An intensive local source (the construction place of an elite residential complex on the site of dismantled and demolished scientific and industrial buildings and services) is located in the immediate vicinity of IAP observation point, 150–300 m in a NW direction. The Balchug weather station is located 800 m in a NE direction from IAP. The Spir MEM point is located 2900 m in a NW direction from IAP, in the courtyard of a multi-storey residential building, close to roads with medium and low traffic loads. The Sukhar MEM point is located 3900 m in a NNE direction from IAP, in

close proximity to a busy highway (Garden Ring road) in the center of Moscow with high traffic of vehicles.

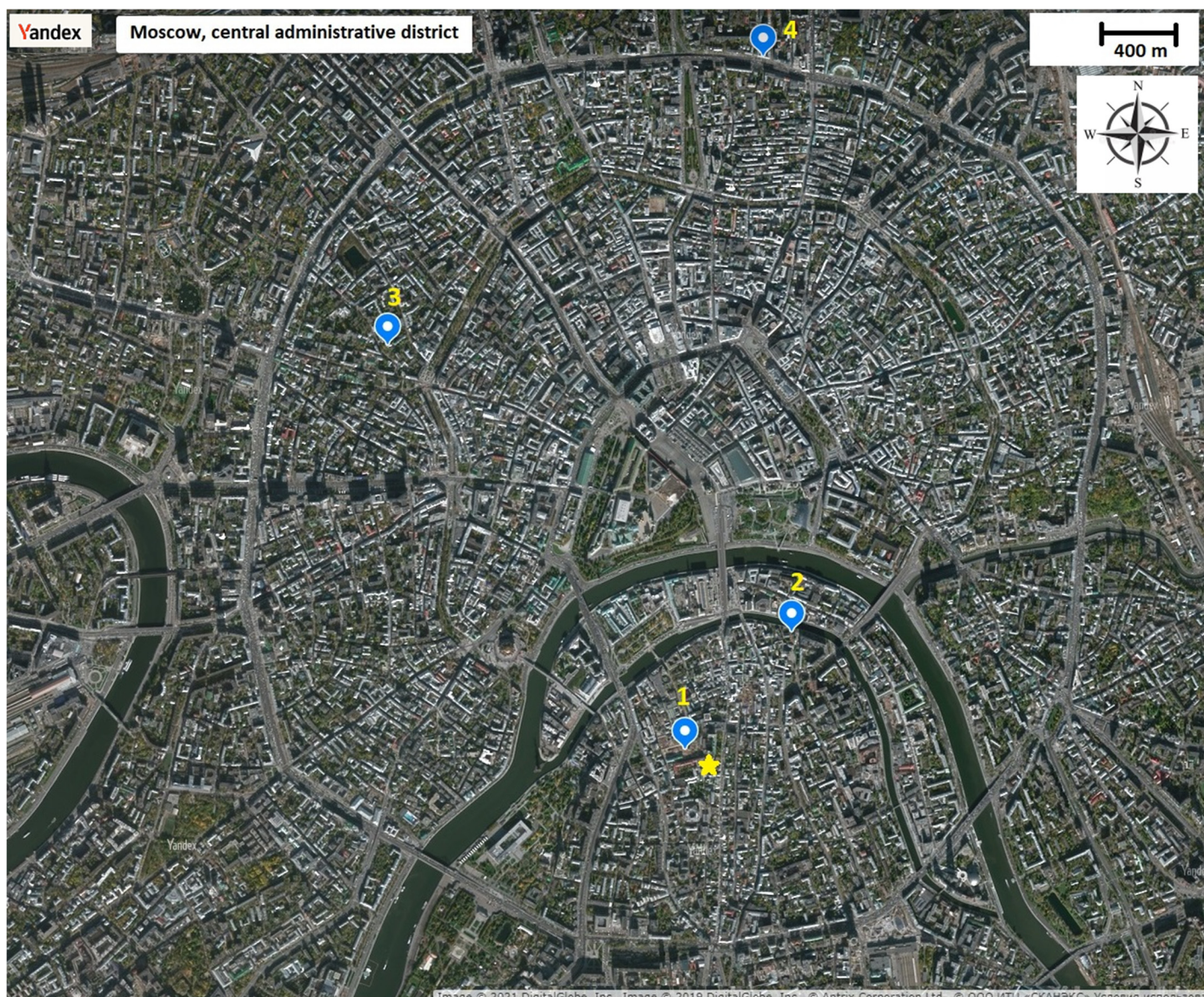


Figure 1. Location of the IAP observation point (asterisk), local anthropogenic source (1), Balchug meteorological station (2), station Spiridonovka (Spir) of the State Research and Development Institution “Mosecomonitoring” (MEM) (3) and station Sukharevskaya (Sukhar) MEM (4) in the center of Moscow.

2.2. The Methods to Studying Aerosols

To determine the microphysical characteristics of the surface aerosol, we used laser and optoelectronic aerosol spectrometers. These devices continuously measure the distribution of the number of particles by size (the number distribution) [2] (p. 353, paragraph 8.1.1) in the diameter range of 0.15–10 μm . Simultaneously with the registration of the number of particles in automatic mode, the distribution of particles by volume (the aerosol volume distribution) is calculated and recorded according to the algorithm embedded in the software of the device [2] (p. 356, formula 8.6). The distribution of aerosol mass by particle size (aerosol mass distribution by size) in the range of 0.15–10 microns was determined by a well-known formula [2] (formula 8.8).

Separately, the total aerosol mass concentration was determined by the gravimetric method, which consists of depositing aerosol particles on the filter from a certain volume of

air, determining the filter weight and calculating the mass concentration value (in $\mu\text{g}/\text{m}^3$), knowing the volume of pumped air.

For gravimetric and elemental analysis, samples were taken by aerosol AFA (Kimry, Russia) filters [73]. These are standard filters made of fibrous material-Petryanov's filtering cloth (PFC). They are designed for highly efficient capture of aerosol of various chemical and sized composition. The capture efficiency is high: the slip coefficient in AFA filter is 0.1% for particles of 0.1 μm in size. In our experiment, AFA filters with a working surface area of 20 cm^2 and at pumping speed of 110–140 L/min were used as part of aspiration samplers.

Our equipment takes aerosol samples daily at a height of about 2 m above the surface, the filter being changed at 9 a.m. Moscow time.

Elemental composition of aerosol particles was studied by laboratory analytical methods: inductively coupled plasma mass spectrometry (MS-ISP), inductively coupled plasma atomic emission spectrometry (NPP-ISP) and X-ray fluorescence analysis (XFA) [74–76]. We analyzed more than 60 chemical elements of various genesis—elements of global distribution, including rare earth and radioactive elements, heavy metals and metalloids, in near-surface aerosol in Moscow.

For interpreting the experimental data obtained, we used open Internet resources [77] and archives of meteorological data [78,79] from weather station Balchug, the closest station to the observation point IAP (for the position of it, see in Figure 1). To analyze long-range atmospheric aerosol transport to Moscow, we calculated the backward trajectories of air mass transport with the help of the HYSPLIT model [80,81] on the website of Air Resources Laboratory (ARL) NOAA (College Park, MD, USA) [82]. For each daily aerosol sample, eight trajectories of 72 h duration starting every 3 h at altitudes of 100 and 250 m have been calculated. The analysis of the fire situation was carried out according to Internet resources [83,84]. The spatial distributions of dust and black carbon (BC) in near-surface air over ETR were analyzed according to MERRA-2 reanalysis data (version 2) [85]. The results of our experiment at IAP in Moscow are compared continuously (daily) with the data of the network stations of the State Research and Development Institution “Mosecomonitoring” (MEM) [86] measuring the mass aerosol concentrations of PM_{10} and $\text{PM}_{2.5}$ particles near-surface aerosol at different points of Moscow (Figure 1).

The experiment was methodically constructed in such a way that for two years of observations, continuous data series were obtained on particle number and mass concentrations of submicron and micron aerosol particles in a range of 0.25–10 microns in near-surface air of Moscow atmosphere. In addition, intensive complex observations (IntObs) were conducted every season for 35–40 days, for which the total aerosol mass concentration (up to 30–40 μm in size) was additionally determined by gravimetric method. Moreover, the elemental composition of near-surface aerosol was also studied during IntObs from the daily aerosol probes collected using aspiration samplers. The first results of our complex experiments were published in [26,65,87,88].

3. Results and Discussion

3.1. Episodes of High Atmosphere Aerosol Pollution, Background Conditions, Seasonal Variations

Figure 2 shows the average daily values of mass aerosol concentration for the particles of smaller than 10 μm (PM_{10}) and less than 2.5 μm ($\text{PM}_{2.5}$) during continuous two-year observations in Moscow (IAP)-from the end of 2019 to November 2021. As mentioned above, the observation point is located in the city center, but away from the most intense and major highways, which makes this point representative for describing a stable background level of atmospheric pollution in the city. Figure 2b shows the data of IAP observation station with similar results obtained at two MEM stations closest to it, Spiridonovka (Spir) and Sukharevskaya (Sukhar), also located in the city center (Figure 1). The location of the station Spir MEM is similar to the IAP station, in alleys, at a distance from active highways. Sukhar MEM is located on a street with heavy car traffic and provides data on the composition of the air in a more urbanized area of the center of Moscow. Despite

these differences, the two-year series of daily measurements of mass concentration of PM₁₀ and PM_{2.5} aerosol particles at all three stations are very close. The values of correlation coefficients of the values of the average daily concentration of PM₁₀ for all qualitatively homogeneous data for two years were 0.87 (between IAP and Spir) and 0.66 (between IAP and Sukhar).

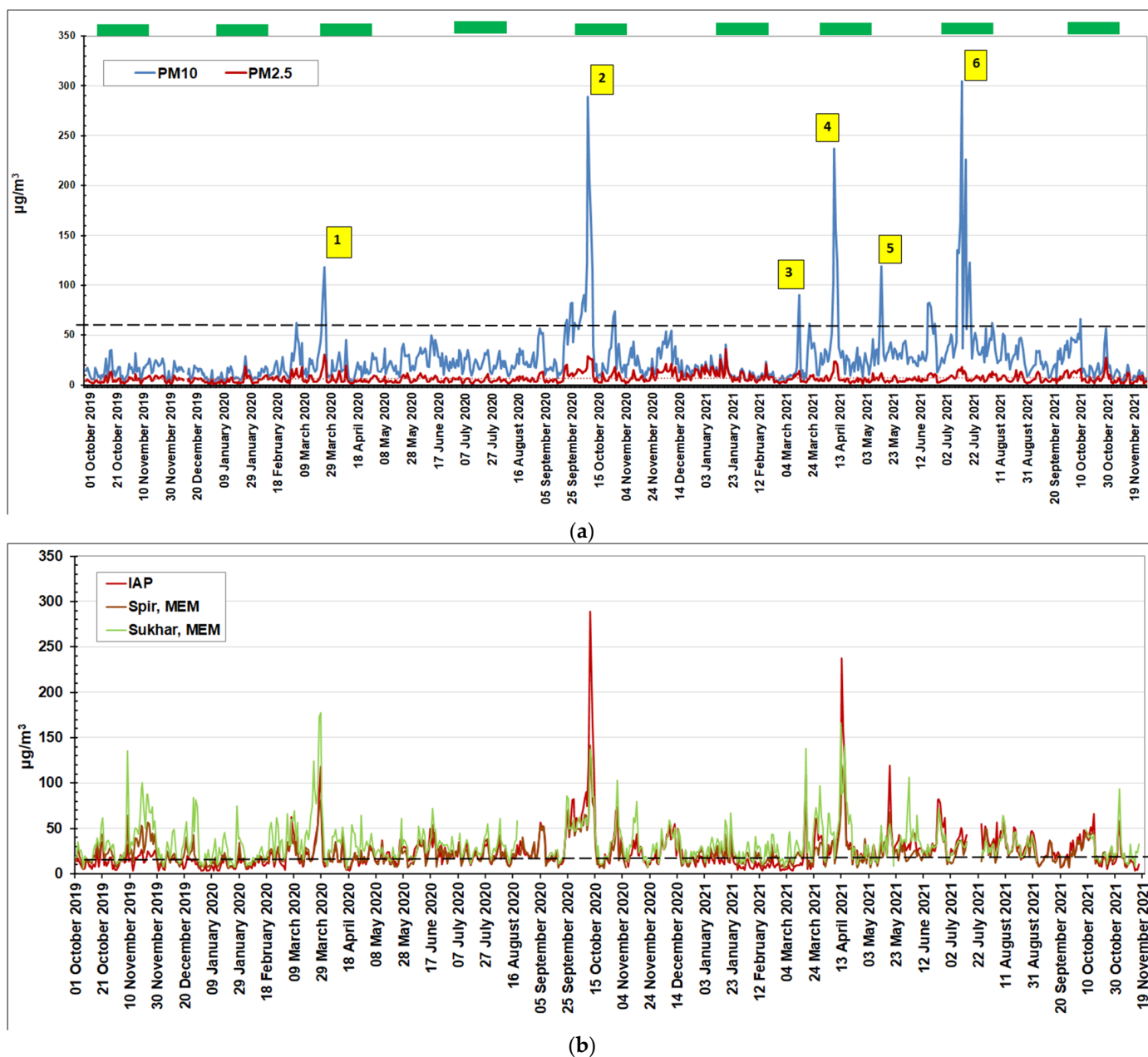


Figure 2. Average daily values of PM₁₀ and PM_{2.5} particles mass concentration in near-surface air in Moscow during two years of continuous monitoring: (a) (upper figure)-selection of episodes for analysis (yellow squares 1–6), green segments at the top—periods of intensive monitoring with determination of aerosol elemental composition; (b) (lower figure)-comparison with the results of monitoring at the MEM stations (Spiridonovka and Sukharevskaya). Dashed lines are the daily MPC value for PM₁₀ particles in the air of residential areas.

As can be seen from Figure 2a, for two years the PM_{2.5} aerosol concentration was below the MPC value (35 $\mu\text{g}/\text{m}^3$, according to Russian standards; 25 $\mu\text{g}/\text{m}^3$, according to World Health Organization (WHO) standards) all the time. For PM₁₀ aerosol, this was almost

always, except for a few episodes with average daily aerosol concentrations significantly above the MPC level ($60 \mu\text{g}/\text{m}^3$, according to Russian standards; $50 \mu\text{g}/\text{m}^3$, according to WHO standards [89]). The total number of such days was 33 for two years, i.e., no more than 5%. In this paper, we will consider in detail six episodes with a PM_{10} mass concentration higher than $60 \mu\text{g}/\text{m}^3$ (MPC value) (see Table 1 and the yellow squares in Figure 2a) in Moscow during these two years—in terms of the conditions of their occurrence and the sources of the urban atmosphere pollution in these cases.

Table 1. Selected episodes with extreme aerosol air pollution in Moscow—at IAP, Spir MEM, and Sukhar MEM. Background—undisturbed level: the average monthly value for the days outside the episodes Nos. 1–5, and the value for Sunday 18 July 2021 without working of the source—for the episode No. 6.

Episode	Period	PM_{10} (Max), $\mu\text{g}/\text{m}^3$			PM_{10} (Background), $\mu\text{g}/\text{m}^3$	
		IAP	Spir, MEM	Sukhar, MEM	IAP	
1	27–29 March 2020	118	82	178	13	
2	10–14 October 2020	290	141	137	19	
3	17–19 March 2021	90	109	138	13	
4	11–15 April 2021	237	120	87	25	
5	17–19 May 2021	119	68	55	28	
6	14–23 July 2021	305	34	38	37	

Table 1 allows us to compare the considered episodes of increased aerosol air pollution by their level of PM_{10} mass concentration with each other and with the background conditions of the month. In particular, a comparison with the background level shows that the air at the MEM stations was also exposed to pollution, as in the IAP observation point, during five episodes (Nos. 1–5). During episode No. 6, the air was extremely polluted only at IAPa, which confirms the locality of the pollution source in this episode.

Since fluctuations in the aerosol concentration values of both fractions consistently occur within the MPC (except for rare extreme episodes), we propose to estimate the background (slightly disturbed) levels of PM_{10} and $\text{PM}_{2.5}$ aerosol concentrations for each month and season in Moscow as average values for, respectively, 1 or 3 months, excluding the days when the concentrations of PM_{10} particles exceeded the MPC value. This should be done separately for each season, since meteorological conditions and the state of the underlying surface are important factors forming the aerosol field in near-surface atmosphere, and the background level should depend on the season. The results of such estimates for PM_{10} and $\text{PM}_{2.5}$ mass concentrations are shown in Figure 3.

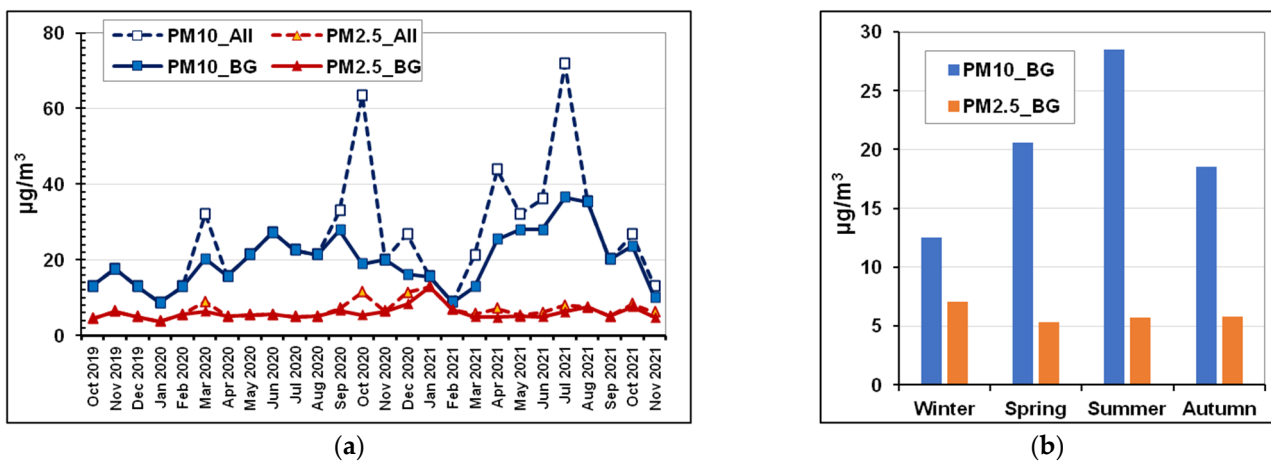


Figure 3. Intra-annual changes in the average (All) and background (BG) values of the aerosol concentration of PM_{10} and $\text{PM}_{2.5}$: (a) by month; (b) by season (on average for two years of observations).

The value of mass concentration of fine aerosols $PM_{2.5}$ changes a little throughout a year. In winter, the intensity of the city’s energy complex is the highest, and the mass of submicron aerosol particles in the air is slightly greater than in other seasons (Figure 3a), especially in the season of 2020–2021, compared to the warm winter of 2019–2020 [90]. Seasonal variations in the city aerosol pollution are manifested in changes of a larger, micron fraction of aerosol particle concentration PM_{10} (Figure 3b). This is due to the seasonal differences in the natural conditions forming the aerosol field in near-surface atmosphere. Here we can list, for example, the differences in the following processes: aerosol emissions from the surface, conditions and rate of aerosol particle deposition onto the surface, meteorological characteristics of the atmosphere (temperature, pressure, humidity and wind speed), temperature inversions in near-surface layer of the atmosphere, etc.

3.2. Meteorological Conditions

The analysis of meteorological conditions revealed some characteristic features shared between episodes of high aerosol pollution and meteorological parameters. Table 2 shows the values of the main meteorological parameters (air temperature, relative humidity and atmospheric pressure at the station level) in different seasons of the year during the episodes under consideration and also for long-term averages. The analysis used archives of meteorological data for the years from 2007 to 2021 at Balchug station (see Figure 1) obtained from the Internet resource [78]. The meteorological characteristics in the Table 2 are compared with the values of PM_{10} aerosol mass concentration (\pm STD). The background (BG) conditions were calculated through the IntObs periods without taking into account the days of the episodes or according to the weekend data from 18 July 2021 for the summer of 2021 (episode No. 6).

Table 2. Meteorological conditions and aerosol PM_{10} concentration (\pm STD) in different seasons: comparison of episodes of extremely high aerosol pollution in near-surface air in Moscow with other periods, the average values through specified periods. The BG conditions were calculated through a period of IntObs excluding the days of the episode or, for the Summer 2021 (episode No. 6), from weekend data of 18 July 2021.

Season	Period	$PM_{10}, \mu g/m^3$	T, °C	P, hPa	U, %
Spring 2020	March–May	23 ± 17	6.9	997	62
	IntObs (25 March–3 May 2020)	23 ± 23	6.1	997	54
	Episode No. 1 (27–29 March 2020)	90 ± 28	9.5	1010	36
	BG conditions	18 ± 11	5.8	996	56
	Long-term average meteo-data for March 2007–2019	–	–0.4	998	69
Autumn 2020	September–November	39 ± 43	9.0	1005	72
	IntObs (1 October–10 November 2020)	53 ± 58	9.2	1004	71
	Episode No. 2 (10–14 October 2020)	128 ± 73	13.5	1008	59
	BG conditions	29 ± 20	7.8	1004	75
	Long-term average meteo-data for October 2007–2019	–	7.1	1002	76

Table 2. Cont.

Season	Period	PM ₁₀ , µg/m ³	T, °C	P, hPa	U, %
Spring 2021	March–May IntObs (25 March–5 May 2020)	32 ± 34	6.9	998	62
	Episode No. 4 (11–15 April 2021)	40 ± 43	7.3	998	61
	BG conditions	156 ± 59	13.3	1005	44
	Long-term average meteo-data for April 2007–2019	28 ± 13	6.7	998	63
	July 2021	–	7.1	1000	60
	Episode No. 6 (14–23 July 2021)	70 ± 67	24.1	998	51
Summer 2021	18 July 2021 without local source	154 ± 70	24.5	996	53
	BG conditions	37	26.2	994	56
	Long-term average meteo-data for July 2007–2019	36 ± 10	23.9	1001	50
		–	21.9	997	60

As can be seen from the Table 2, episodes of high aerosol pollution in spring and autumn are characterized by concentrations of PM₁₀ $C_{EPI} > (C_{BG} + 3 * STD_{BG})$. They are accompanied by increased values of temperature and pressure, as well as reduced humidity in near-surface air. The meteorological parameters of episode No. 6 practically do not differ from the monthly average values and from the average background values (indexed BG) outside the episode.

Figure 4 shows wind roses calculated for months with episodes of extreme aerosol pollution in comparison with long-term (2007–2019) average ones. The top four diagrams (Figure 4a) refer to episode 1, then two down-episodes 2 (Figure 4b), 4 (Figure 4c) and 6 (Figure 4d). All episodes of high aerosol concentration in near-surface air of Moscow occurred in months with wind roses differed from the long-term average one, with the exception of episode 6, when air pollution depended on a close local anthropogenic source, and not on meteorological conditions. It is also interesting to note that in the months with increased air pollution, the percentage of calm conditions was higher than the long-term average one, especially in October 2020.

The wind speed in the atmosphere near the surface in the center of Moscow rarely exceeds 3 m/s in single measurements. The average daily value of wind speed is usually 1–2 m/s. Comparing the percentage of calm in certain months of 2020 and 2021 with the long-term average ones (Figure 4), we can suppose that the probability of calm conditions in the center of Moscow has increased in recent years.

The study of the dependence of the aerosol PM₁₀ mass concentration on atmospheric air pressure in the near-surface atmosphere in Moscow showed that an increase in atmospheric pressure accompanies not only episodes of high aerosol pollution. In undisturbed (BG) conditions, outside of the episodes of extreme increase in aerosol concentration, PM₁₀ aerosol mass concentration in the near-surface atmosphere also increases (Figure 5). This may be caused by anticyclonic conditions with descending air flows (and aerosols in them), as well as with a weakening of aerosol, which sink onto the surface due to a decrease in air humidity, often accompanied by an increase in pressure. The PM₁₀ aerosol mass concentration in near-surface atmosphere also increased when the air temperature goes up, during the transition seasons (spring and autumn). The simplest mechanism of this connection may be an increase in soil/dust emissions into the atmosphere when the underlying surface dries at a higher air temperature.

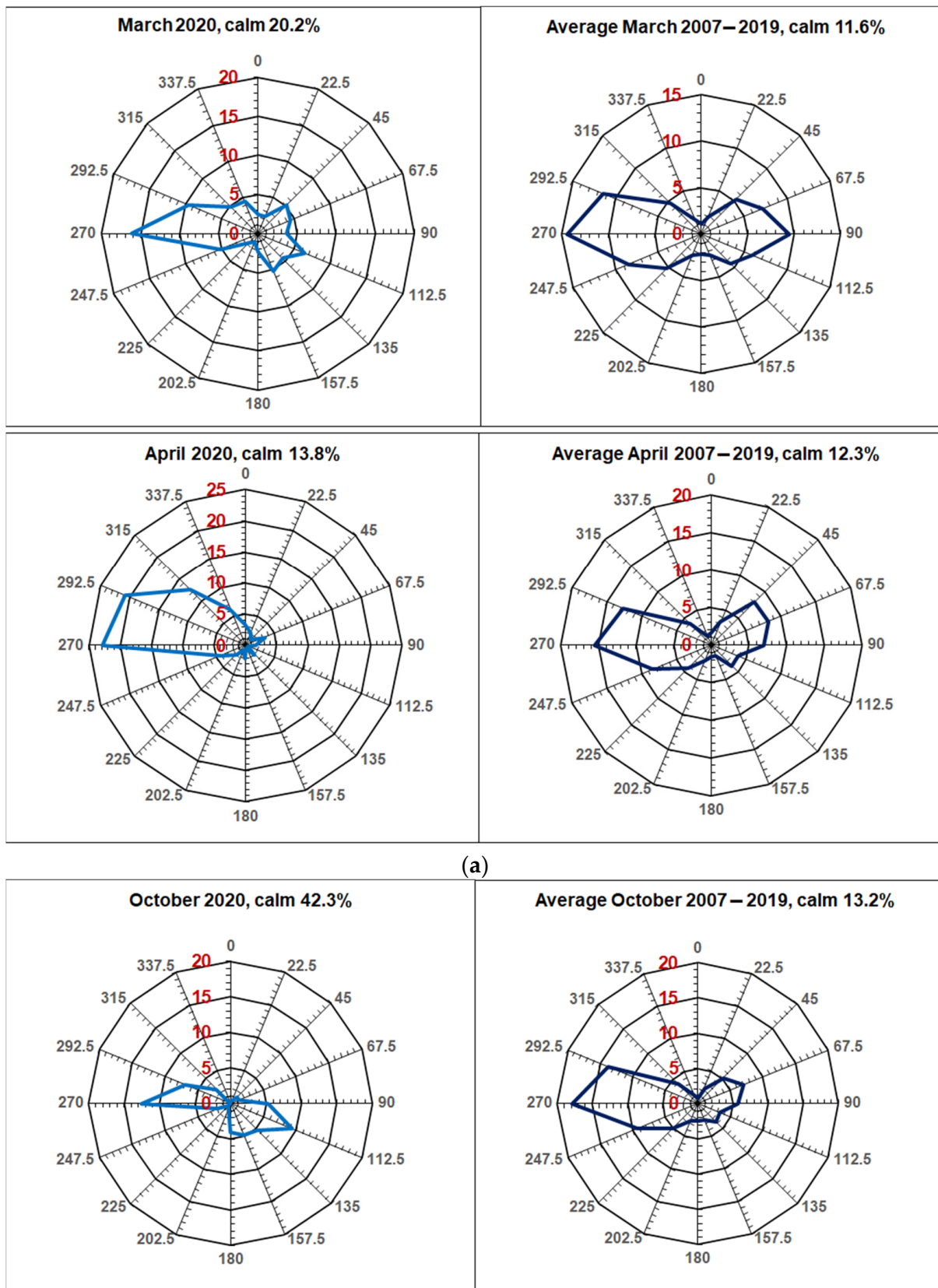


Figure 4. Cont.

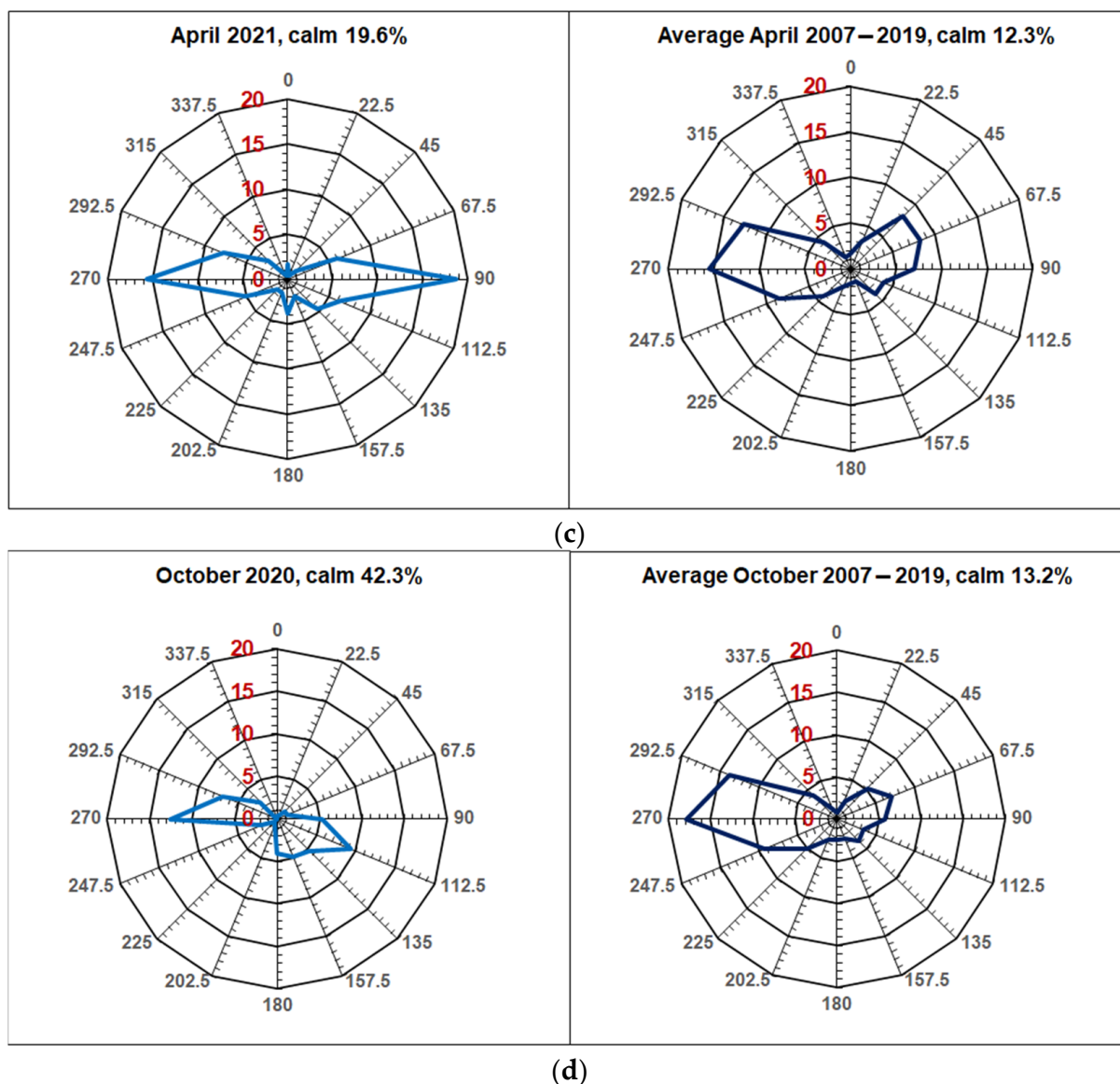


Figure 4. Wind roses: on the left—the average for the month; on the right—the average for the same month for 2007–2019. The percentage of calm conditions is indicated on each picture. The series of diagrams (a–d) refer to the episodes 1, 2, 4, 6 (Table 1 and Figure 1), respectively.

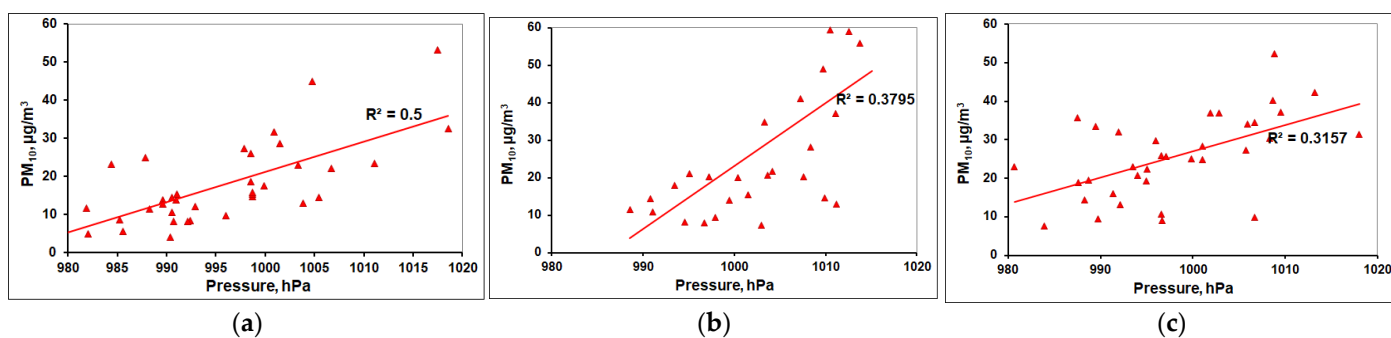


Figure 5. The dependence of the PM_{10} aerosol concentration on the air pressure in the surface atmosphere in Moscow during periods of intensive observations through the days outside the episodes of maximum air pollution (Table 2): (a) spring 2020; (b) autumn 2020; (c) spring 2021. R^2 —the reliability coefficient of the linear relationship (straight lines) between variables.

3.3. Spring Episodes of Maximum Air Pollution Due to Atmospheric Transport of Biomass Burning Aerosols from the Regions with Biomass Fires to Moscow

All cases of exceeding the MPC level by the values of PM_{10} concentration in the air of Moscow (Figure 3) are associated with aerosol transport from remote (episodes No. 1–5) or local sources (episode No. 6) to the observation point. The situation usually worsens and the concentration of aerosols increases under high atmospheric pressure, as well as with temperature inversions in the surface layer of the atmosphere. As a rule, the end time of the episode is associated with a change in the synoptic situation: a change in the direction of air mass transport and/or air cleaning with increased in humidity and precipitation.

The episode No. 1 of extremely high aerosol pollution (Figure 2 and Table 1) was in the days of air mass transport to Moscow from the regions with intensive biomass burning around Moscow and from the other mid-latitude regions. The examples of such transport are shown in Figure 6 on the distribution maps of fire centers (from [83]), as well as in Figure 7a,b—on the maps of BC mass concentration distribution (as an indicator of biomass burning) in the surface atmosphere, according to MERRA-2 reanalysis data [85].

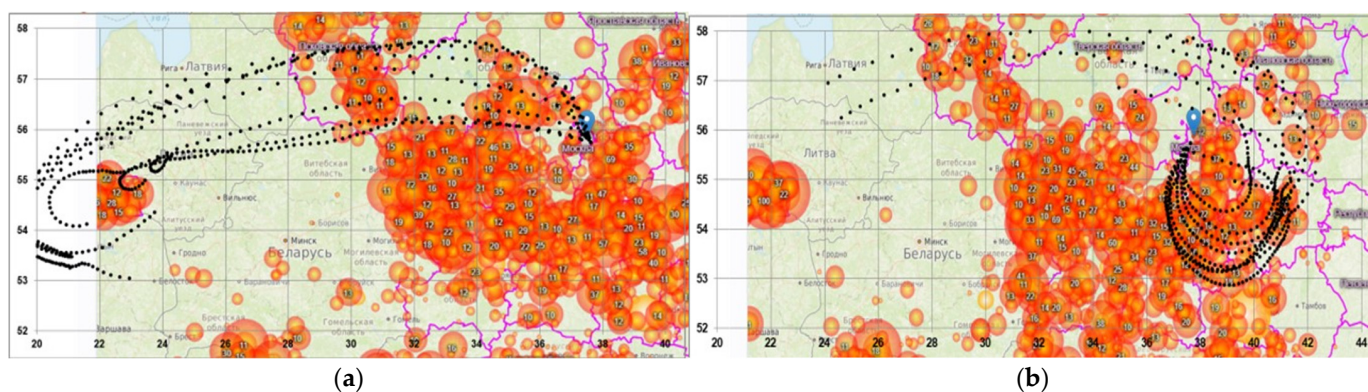


Figure 6. Examples of fire distributions in near-surface atmosphere over ETR territory (according to the data [83]) and trajectories of air mass transport (black dots) to Moscow (blue flyer) for 26 March 2020 (a) and 28 March 2020 (b) of the episode No. 1 of high aerosol pollution.

Figures 6 and 7 shows examples of air mass transport trajectories to the IAP observation point in Moscow constructed using the NOAA HYSPLIT model [80–82] for episodes No. 1 (25–29 March 2020) and No. 4 (11–15 April 2021), see Figure 2 and Table 1.

During these episodes, aerosol particles were transported in the atmosphere from nearby areas with numerous biomass burning points. They could be landfills burning after winter, last year's tops and grass burned in the fields, etc. Moreover, the spring of 2020 was unusual early (after an unusual short, warm and low-snow winter—see the Table 2 and [90]); therefore, significant fires in the region began in March. According to the results of long-term studies [91,92], the characteristic seasonal maxima of PM_{10} and $PM_{2.5}$ concentrations for Moscow region is observed in April, as it happened in 2021 (Figure 3a). As can be seen from Figure 7, the sources of biomass burning aerosols may be located closer or farther from Moscow, from different sides of it. On some days, in accordance with the atmospheric circulation regime, these impurities are transported by air advection in Moscow, fundamentally changing the level of city air pollution, so that the concentration of PM_{10} particles exceeds the MPC value.

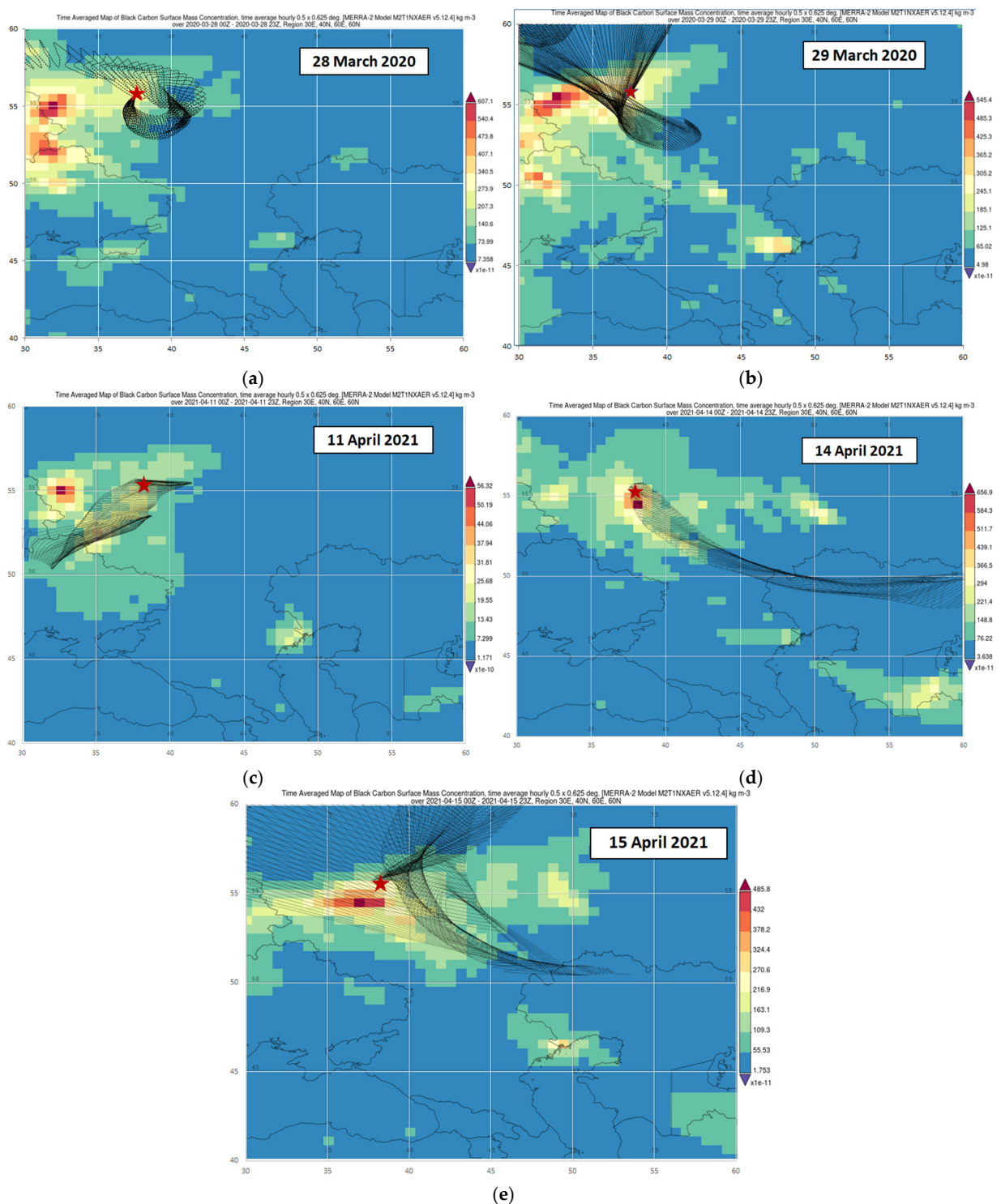


Figure 7. Examples of BC distributions (as an indicator of fire emissions) in near-surface atmosphere over ETR territory (according to MERRA-2 reanalysis [81]) and trajectories of air mass transport (black dots) to Moscow (asterisk) for individual days from episodes No. 1 (a,b), No. 4 (c–e). The color scales of BC concentration on the maps are different, kg/m^3 .

3.4. Episodes of Maximal Air Pollution during Atmospheric Transport of Dust and Sand to Moscow from the Regions with Dust Storms

In addition to fire aerosols, the reason for the increase in aerosol concentration in near-surface atmosphere of Moscow, as mentioned above, may be the long-range transport of dust and sand from the areas of dust storms in the south-east of the ETR, on the Caspian Sea

coast, and in western Kazakhstan [27]. An example of such an impact on the composition of the Moscow air is episode No. 2 (5–15 October 2020)—Figure 2 and Table 1. The trajectories of long-range air mass atmospheric transport to Moscow and the distribution of dust in the surface atmosphere during this period are shown in Figure 8. During the days of high PM₁₀ aerosol concentration in Moscow, air masses moved to the city from arid and desert areas near the Caspian Sea, in Kalmykia, and in the lower reaches of the Volga River.

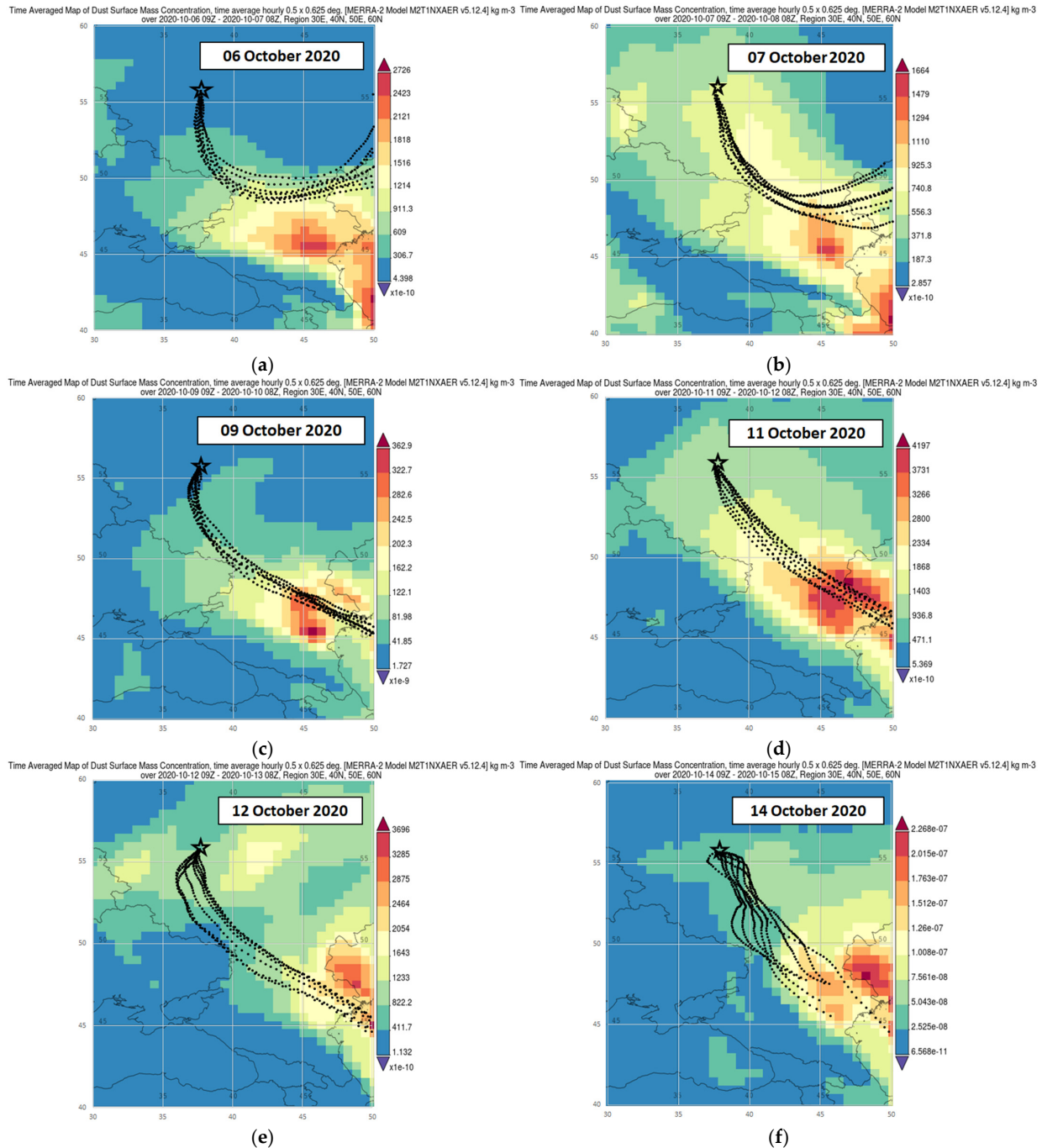


Figure 8. The development of the episode No. 2 (5–15 October 2020): examples of dust propagation (as an indicator of dust storm emissions) over the territory of the southern half of ETR (according to MERRA-2 reanalysis [81]) and air mass transport trajectories (black dots) to Moscow (asterisk) for individual days from 6 to 14 October 2020 (the dates are shown in the pictures). The color scales of dust concentration on the maps are different, kg/m³.

In general, the process of spreading aerosols to Moscow from the areas of dust storms in the south-east of ETR and in western Kazakhstan is a rather rare phenomenon. Estimates of the works [66–68] show that the probabilities of such air mass transport in different seasons until 2017 did not exceed 5%. However, during the two years of observations considered in this paper, such episodes of varying duration occurred regularly in spring and autumn. Even in winter, at the beginning of December 2020, we found a steady (longer than a week) aerosol transport from these areas to Moscow. As a result, there was an increase in PM_{10} aerosol mass concentration up to the levels close to the MPC value in Moscow [90]. Analysis of the statistics of these phenomena, as well as the dynamics of atmospheric processes that cause and accompany them, is still to be done. As possible explanations, it can be assumed, for example, that in recent years, due to climate changes on the planet, dust storms in the Caspian semiarid and arid zones have become more frequent and more powerful. So far we have not been able to find literature on the statistics of dust storms in the Caspian region. This is also possible due to changes in atmospheric circulation processes in such a way that the air mass transport from arid and desert areas of the Caspian Sea to the ETR center has become more frequent. This assumption should be verified by analyzing long-term (including recent years) data on the ways of air mass transport to Moscow. The simplest reason for the lack of publications about such a phenomenon may be that two years ago there were only few episodic and sporadic measurements of aerosol composition in Moscow, and such rare extreme episodes could not get into them.

Figure 9 shows the situations that developed during the short and not too strong episodes of increasing aerosol pollution—No. 3 (15–19 March 2021) and No. 5 (17–19 May 2021). In May 2021 (Figure 9a), for a short episode, aerosols of arid origin from the desert east of the Caspian Sea arrived in Moscow. The concentration of PM_{10} aerosols exceeded the MPC value for one day. Mixed cases of long-range aerosol transport to Moscow from fire and dust areas in the southeastern part of ETR are also possible (Figure 9b,c), as it was in March 2021.

The pictures of Figure 9 show that the air masses moving towards Moscow could capture impurities from the areas of biomass burning both near the city itself, and in the north-west of the Caspian Sea or in Kalmykia (Figure 9c). At the same time, aerosols formed in places of dust storms east of the Caspian Sea could enter into the same air masses (Figure 9b). As such, mixed arid and smoke aerosol was apparently registered in Moscow. Unfortunately, this episode was short and did not coincide with the intensive monitoring of the aerosol composition in Moscow in the spring of 2021, when the elemental composition of the aerosol was measured.

3.5. Extreme Air Pollution under the Influence of the Local Anthropogenic Source

A record increase in the concentration of ground-level aerosol was recorded at IAP observation point in episode No. 6 from 14 July to 23 July 2021 (Figures 2 and 10 and Table 1). However, as can be seen in Figure 2b, this episode did not affect the measurements of Spir. MEM and Sukhar. MEM stations in any way, in contrast to the episodes associated with the long-range transport of aerosol to Moscow. These days, the dismantling and demolition of buildings and structures for scientific and industrial purposes was carried out on the territory located in 100–300 m to the west-northwest from the observation point. During this episode, the maximum single and average daily mass concentration of PM_{10} aerosol at IAP observation point repeatedly exceeded MPC value (by 2–5 times), and the amount of mass concentration at Spir. MEM (by 3–9 times) [65]. The synoptic situation (the influence of a high blocking anticyclone) and unfavorable meteorological conditions (high and record air temperature in Moscow, calm or quiet wind) contributed to accumulation of aerosol particles in near-surface layer of the atmosphere and increased the effect of local aerosol pollution near the IAP observation point. It should be noted that at the same time, the concentration of $PM_{2.5}$ particles changed slightly (Figure 2a), which fits well into the picture of atmospheric pollution by larger particles formed during the destruction of buildings.

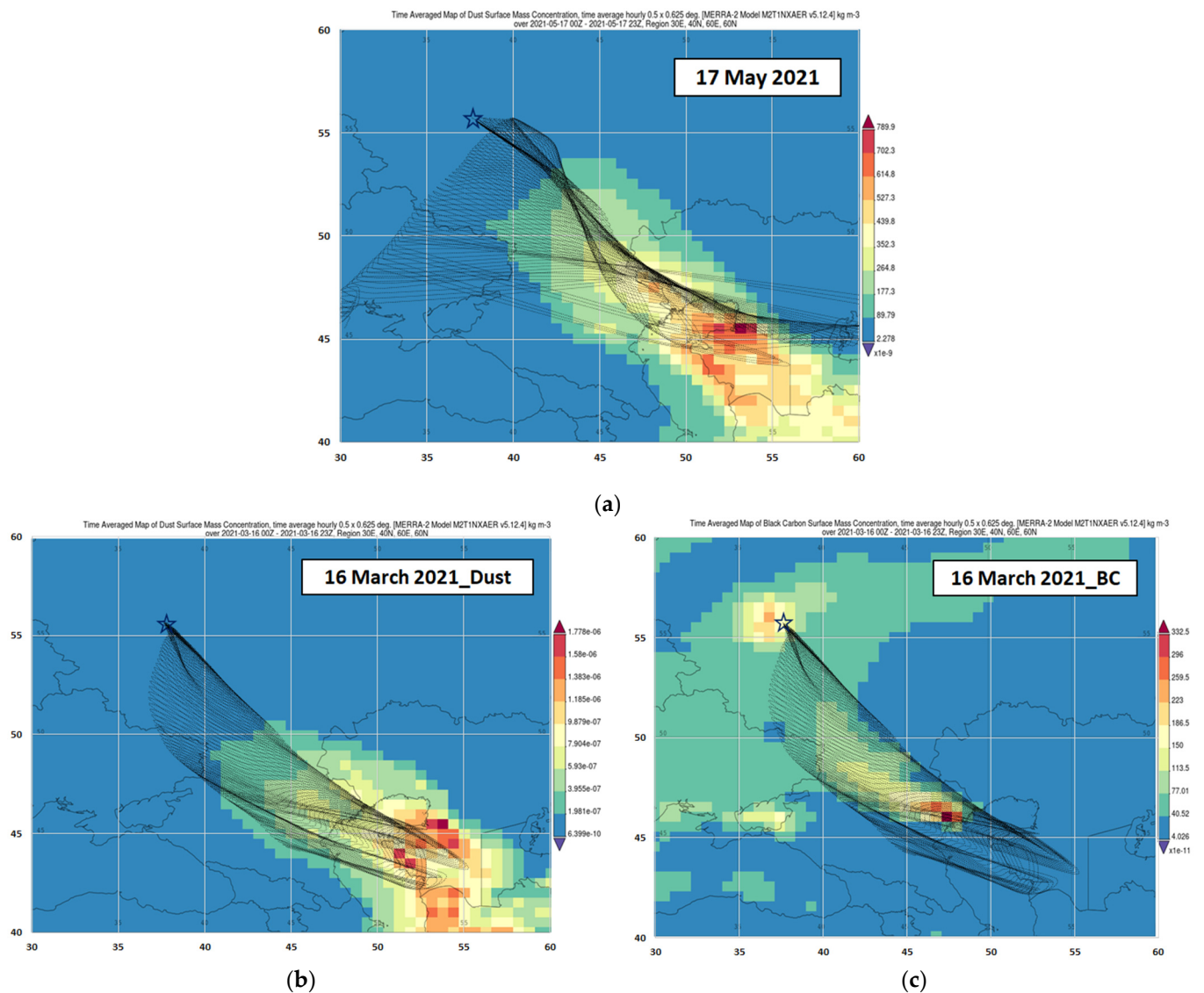


Figure 9. Long-range air mass transport to the Moscow region on 17 May 2021 (a) or 16 March 2021 (b,c). Distributions of dust (a,b) or BC (c) in near-surface atmosphere on the maps correspond to the MERRA-2 reanalysis data [81]. The color scales of BC and dust concentrations on the maps are different, kg/m³.

Here is an approximate estimate of the power of a local anthropogenic source of dust aerosol. A detailed description of the calculations is presented in [65]. Initial data: the distance from the source to the observation point is 300 m, the wind speed is 1 m/s in the direction from the source to the observation point, the measured concentration of PM₁₀ aerosol at the observation point is 300 µg/m³, the height of the mixing layer $H = 100$ m. Assuming that the removal of impurities from the atmosphere is carried out by dry deposition to the surface and is described by an exponential dependence on time, the mass of the aerosol in the air above the source area of 1 m² is 31.4 mg. The emission of dust aerosol into the atmosphere from 1 m² of such a local surface source ranges from 0.56 to 0.80 kg/day/m² at 5–7 h of operation per day. This substance is dispersed around the source, depending on the variability of wind direction and speed, at distances up to 3–5 km (at an aerosol deposition rate of about 3 cm/s for particles up to 10 µg in summer dry time). When the source turns off, the air near the source will be purified to the level of 10–40% only after 50 min or more, to the level of MPC value in 0.5–1.5 h. Of course, these rough estimates in the city may be somewhat overstated due to the complexity of

the relief of urban development. However, the opposite cases are also possible—due to the formation of urban street canyons with increased wind speed. In addition, the uneven distribution of the impurity in height in the near-surface atmosphere, complex mixing processes of the impurity at heights exceeding the heights of neighboring buildings, vertical convection, spreading of the impurity flow horizontally and other processes significantly complicate calculations.

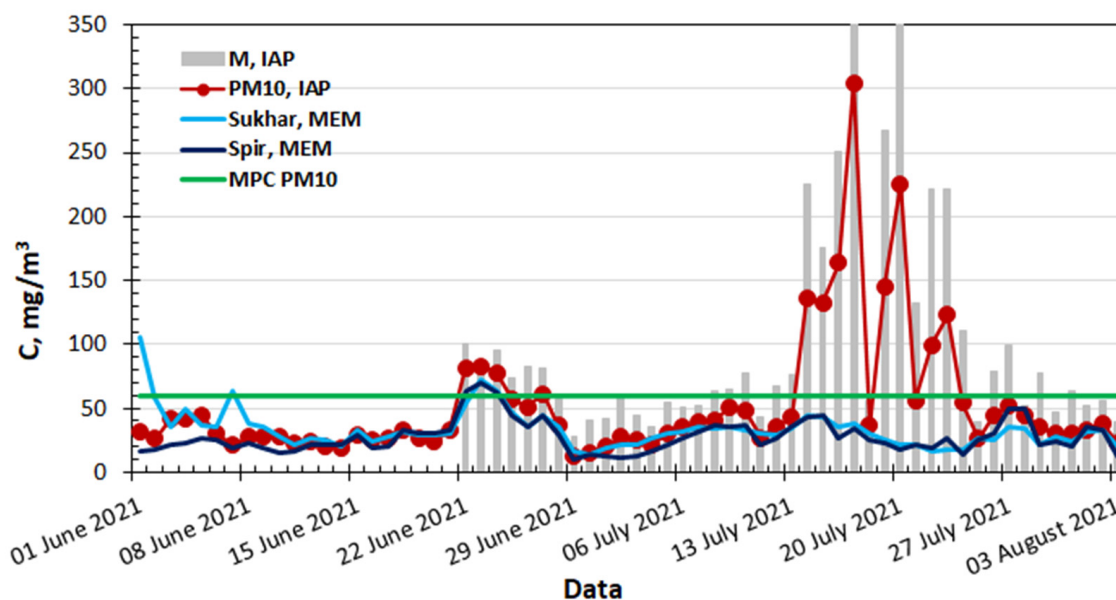


Figure 10. The average daily mass concentration of PM_{10} particles and the total aerosol mass (M) in the summer of 2021 before, during and after episode No. 6 of extreme aerosol pollution (according to observations by IAP and MEM). The green line indicates the MPC value for daily PM_{10} mass concentration.

In general, the analysis of episode No. 6 and its comparison with other episodes reviewed above show that an intense local anthropogenic source may be comparable in duration and amplitude of the impact with the effect of dust storms in the arid regions, the aerosol from which is sometimes recorded in the Moscow region. During the period of 2 years of continuous observations at IAP, this episode was characterized by extreme aerosol pollution of near-surface atmosphere of the center of the metropolis, and the daily concentration of near-surface aerosol, regardless of weather and meteorological conditions, strongly depends on the operating mode and power of the local source.

3.6. Elemental Composition of Near-Surface Aerosol during the Periods of High Atmospheric Aerosol Pollution in Moscow

The elemental composition of aerosol particles is the most important parameter of an aerosol, not only affecting the chemical composition and chemical activity of the atmosphere, but also being a marker of aerosol sources of various origin [93]. However, the study of the elemental composition is a very time-consuming process that requires a high degree of purity of the experiment and is also associated with a very expensive analysis of aerosol samples. Apparently, this is why there are few publications in the world literature about the elemental composition of aerosols, especially in cities. It is possible to name individual articles devoted to the study of aerosol elemental composition in different regions of Russia, for example, [94–97] and the world, for example, [98–108]. As for the atmosphere of the Moscow region, studies of elemental composition were carried out there only sporadically, and there are few published works on this topic, in particular, [25–27,87,88,109,110].

In this paper, the aerosol elemental composition is analyzed during the considered episodes with an abnormally high aerosol concentration in Moscow, taking into account background (conditionally introduced by us) geochemical profile of the elements for each

episode. Background for elemental concentrations is calculated in the same way as for PM_{10} and $PM_{2.5}$ mass concentrations (see above, Section 3.1) from the data excluding the episode. In total, 65 chemical elements (from Li to U) were determined in aerosol daily samples in different seasons. For a convenient presentation of the results, we consider 33 elements representing four groups of elements in accordance with known classifications [111–116]: elements of global distribution, heavy metals and metalloids of terrigenous and/or anthropogenic origin, and radioactive elements.

In Figure 2a at the top, the green segments highlight the periods when, once in each season (for 35–40 days), a comprehensive monitoring of aerosol composition was carried out with aerosol sampling to analyze the concentrations of chemical elements included in it. Three episodes related to the long-range atmospheric transport of aerosols to Moscow from the areas of fires and sandstorms—the episodes Nos. 1, 2 and 4 (Figure 2a)—have the data on elemental aerosol composition, as well the data on the total aerosol mass M . Besides the absolute values of an element X concentration C_X , we will analyze its enrichment factors EF_X relative to the composition of the Earth's crust (average composition of the Earth's crust from [116], reference element La), calculated as follows:

$$EF_X = (C_X/C_{La})^{AER} / (C_X/C_{La})^{CRUST}. \quad (1)$$

Figure 11a,b shows the concentration and EF profiles for selected 33 elements under consideration. These distributions are similar not only for background conditions, but also for episodes of high atmospheric pollution in the city, which is explained by the overall regional content of the elements in question in the atmosphere above ETR. The more subtle differences manifested mainly for the elements of local origin, including anthropogenic elements in the city.

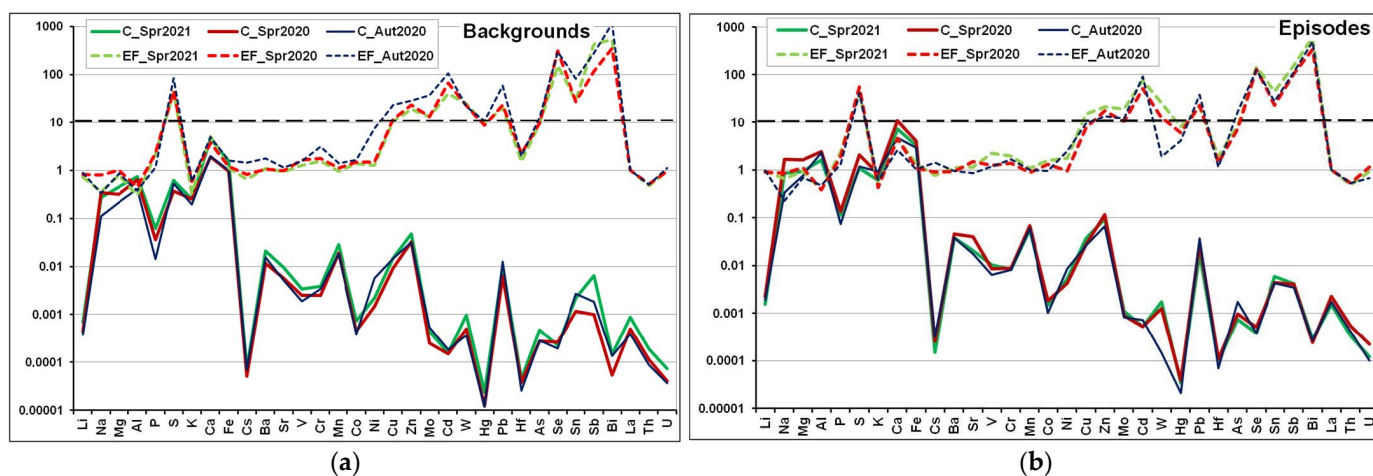


Figure 11. Comparison of elemental composition of near-surface aerosol for three episodes of high aerosol air pollution in Moscow (spring 2021, spring 2020 and autumn 2020) associated with atmospheric transport of pollutants from other areas: (a,b)—concentration C ($\mu\text{g}/\text{m}^3$) and enrichment factor EF (formula 1) of elements under background and episode conditions, respectively. Black dashed lines are the level of $EF = 10$.

Usually, the elements for which $EF > 10$ are considered as non-terrigenous, and the rest are of terrigenous or of mixed terrigenous/anthropogenic origin. Based on this criterion, non-terrigenous elements in Moscow include S, Cu, Zn, Mo, Cd, W, Hg, Pb, As, Se, Sn, Sb and Bi. Since the absolute values of elemental concentrations and enrichment factors may differ by several orders of magnitude (logarithmic vertical scale in Figure 7a,b), consider the relative excess ΔC in concentration of element C during the episode C_{EPI} compared

with the background level of its concentration C_{BG} (outside the episode) for the same monitoring period:

$$\Delta C = (C_{EPI} - C_{BG})/C_{BG}. \quad (2)$$

Let's compare these indicators for three episodes under consideration (Figure 12).

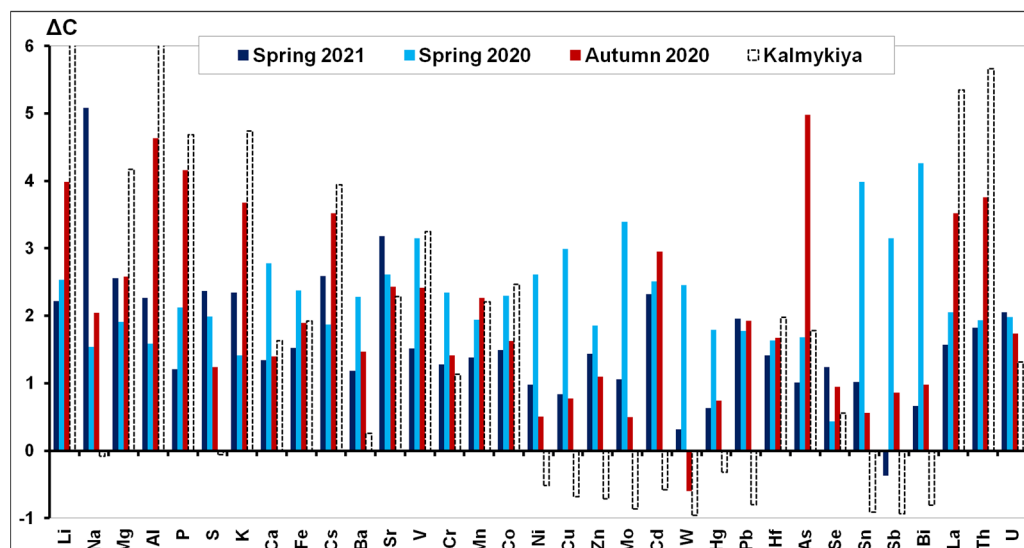


Figure 12. The relative excess of elemental mass concentrations ΔC (formula 2) compared to the background (BG) level (see the text) during three episodes, as well the relative excess of elemental concentration for Kalmykia arid aerosol [27] compared to the background elemental concentrations for autumn 2020 in Moscow.

The profiles of excess elemental concentrations for background levels in the springs of 2020 and 2021 are not similar to each other, as one would expect. This may be explained by different natural weather conditions in the cold seasons of these years, which were discussed above. Moreover, these profiles are in some sense opposite, as indicated by the negative sign of the correlation coefficient in variations from element to element between these seasons -0.38 . Analysis of long-range air mass transport to Moscow during abnormally high aerosol air pollution in the fall of 2020 showed (Figure 8) the effect of dust storms in the southeastern desolate areas of ETR on the aerosol composition in the city. Figure 1 also includes a diagram of the profile of excess elemental concentrations for the aerosol of Kalmykia compared to the background level of elemental concentrations in Moscow in the autumn of 2020. The elemental composition of Kalmykia aerosol was determined from the samples taken during field expedition at the end of July 2020. Figure 12 shows that the profiles of aerosol elemental composition in Moscow in the fall 2020 and in Kalmykia correspond well to each other, especially for terrigenous elements. The correlation coefficient of these element concentration profiles is equal 0.82. This shows the relationship between Moscow aerosol composition and Kalmykia aerosol composition during the episode in Moscow in October 2020.

Figure 13 shows the geochemical profiles of elements in the composition of a surface aerosol during an episode of extreme aerosol pollution in July 2021 under the influence of close local source. Geochemical profiles are presented in relative units (Formula (2))—the relative excess in the element mass concentration ΔC in the days with the highest intensity of the local source compared to C_{BG} on Sunday 18 July 2021 (chosen as a background, in undisturbed conditions, with a non-working local source).

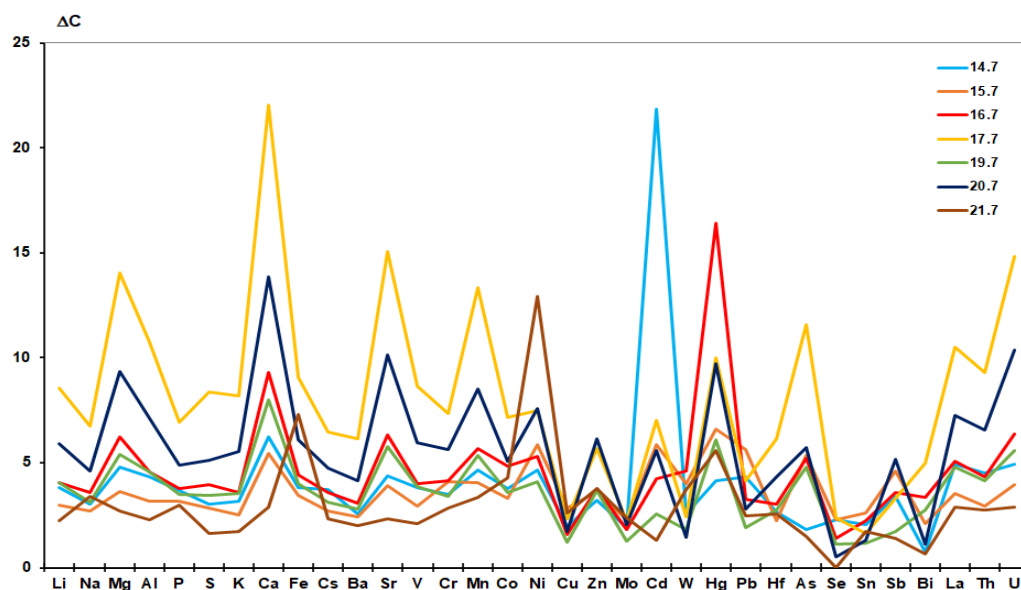


Figure 13. The relative excess of elemental mass concentrations ΔC (formula 2) for the different days of episode No. 6.

The analysis of elemental composition of near-surface aerosol in Moscow during episode No. 6 in July 2021, under the intense influence of local anthropogenic source, showed that the average daily mass concentration of calcium exceeded the MPC ($10 \mu\text{g}/\text{m}^3$), and the concentrations of Fe and Al were slightly below their MPC levels (40 and $10 \mu\text{g}/\text{m}^3$, respectively) [117]. High concentrations of a number of individual chemical elements of terrigenous and technogenic genesis, in particular, Ni, Cd and Hg, were also recorded on individual days.

4. Conclusions

In this paper, the study of the composition of near-surface aerosol in Moscow was carried out based on the results of 2 years of complex field observations in 2020–2021. It was found that during these two years, the average daily mass concentration of aerosol particles $\text{PM}_{2.5}$ did not exceed the MPC value ($35 \mu\text{g}/\text{m}^3$, according to Russian standards) and shows insignificant fluctuations regardless of the season (with only a slight maximum in winter), meteorological conditions or features of natural and anthropogenic sources of pollutants. Noticeable seasonal variations in aerosol pollution in Moscow atmosphere with a maximum in the spring-summer period were manifested in the variability of the mass concentration of a larger, micron fraction of aerosol particles, which is part of the aerosol PM_{10} . Such difference between PM_{10} and $\text{PM}_{2.5}$ aerosols is associated with seasonal features of aerosol forming conditions in the near-surface atmosphere. These may be due to differences in the following processes: aerosol emissions from the surface, conditions and rate of its deposition onto the surface, meteorological characteristics of the atmosphere (temperature, pressure, humidity and wind speed) and the surface, temperature inversions in near-surface layer of the atmosphere, etc.

Several episodes of unusual high mass concentration of PM_{10} particles were recorded, which exceeded the daily MPC value ($60 \mu\text{g}/\text{m}^3$, according to Russian standards) by 3 STD for the period of observations. The total number of such days of extreme aerosol pollution for two years was no more than 5%.

All cases of extremely high aerosol pollution in near-surface air in Moscow were differentiated into six episodes depending on the sources and composition of aerosol particles, taking into account weather and meteorological conditions. The analysis of each of the episodes revealed the following sources of increased aerosol concentration in Moscow:

- regional transport of aerosols from the areas with numerous biomass fires in the spring;

- long-range transport of dust aerosol from arid areas of the south of ETR with intense dust and sand storms;
- mixed transport of fire and dust aerosols from the areas with fires and dust sources under certain weather conditions;
- local powerful anthropogenic source of anthropogenic dust (for example, the process of demolition of industrial buildings).

Episodes of extremely high aerosol concentrations associated with atmospheric transport of pollutants to Moscow from other regions were accompanied by an increase in pressure and temperature, weak wind and frequent calm in near-surface air of the city.

Based on the results of complex studies, the elemental composition of near-surface aerosol in Moscow was determined during the episodes of extremely high aerosol pollution and in background conditions through the days outside the episode. The enrichment factors of chemical elements in Moscow aerosol in comparison with the composition of the Earth's crust were calculated. The non-terrigenous origin of such elements as S, Cu, Zn, Mo, Cd, W, Hg, Pb, As, Se, Sn, Sb and Bi in Moscow has been established. The profiles of elemental mass concentrations, as well of the enrichment factors are similar not only for background conditions, but also for episodes of maximum atmospheric pollution in the city. This is associated with the general regional content of the elements under consideration in the atmosphere above ETR. The differences relate mainly to elements of local origin, including anthropogenic elements in the city.

Profiles of excess concentration of chemical elements in episodes with extreme aerosol pollution above background levels are calculated. The correlation of these profiles for the spring periods of 2020 and 2021 (with the regional transport of fire aerosols) is weak and negative (the correlation coefficient is equal to -0.38). This may be due to different natural weather conditions in the cold seasons of these years, as well as different types of burnt biomass and other features of sources of aerosol pollution.

For the autumn episode of 2020 (long-range dust aerosol transport), the profile of mass concentrations in near-surface aerosol in Moscow was compared with the profile of the elemental mass concentrations of arid aerosol in Kalmykia. A significant correlation between them has been established, especially for terrigenous elements. The correlation coefficient of the profiles of excess elemental concentrations over the background was 0.82. It shows a reliable relationship between the compositions of Moscow aerosol and Kalmykia one during the episode in October 2020 in Moscow.

In July 2021, under the intense influence of a local anthropogenic source, there was a significant increase in concentrations of the most chemical elements compared to background conditions (in the absence of a local source) in Moscow. At the same time, the average daily mass concentration of Ca exceeded its MPC value, and the concentrations of Fe and Al were slightly below their MPC levels. Additionally, on some days, high concentrations of a number of technogenic chemical elements were recorded, in particular, of Ni, Cd and Hg.

In general, the analysis of all episodes of abnormally high aerosol pollution of near-surface air in Moscow showed that an intensive local anthropogenic source is comparable in duration and impact intensity with the effect of dust storms in the arid regions of the south of ETR. During two years of continuous observations at IAP, this episode was characterized by extreme atmospheric aerosol pollution in the center of the metropolis. The daily course of near-surface aerosol concentration, regardless of weather and meteorological conditions, strongly depends on the mode of operation and the power of the local source.

Author Contributions: Idea initiation, D.P.G. and A.A.V.; methodology, D.P.G., A.A.V. and M.A.I.; data collection, D.P.G. and A.I.S.; sample collection, D.P.G. and M.A.I.; sample lab analysis, D.P.G. and M.A.I.; statistical analysis, A.A.V., M.A.I. and A.I.S.; formal analysis, M.A.I. and A.I.S.; investigation, D.P.G. and A.A.V.; data curation, D.P.G.; writing—original draft preparation, A.A.V. and M.A.I.; writing—review and editing, D.P.G.; visualization, D.P.G. and A.A.V. All authors have read and agreed to the published version of the manuscript.

Funding: The work was supported by the Russian Foundation for Basic Research, project no. 19-05-50088 (study of near-surface aerosol composition in Moscow), and by the Russian Science Foundation, project no. 20-17-00214 (study of arid aerosol composition in Kalmykia).

Data Availability Statement: Data sets for this research are publicly available. Archives of meteorological parameter data are available at: Weather archive. <http://weatherarchive.ru/Pogoda/Moscow> (accessed on 12 January 2022), Reliable prognosis. <https://rp5.ru> (accessed on 16 December 2021). Visualization of short-term weather forecasts and synoptic conditions is presented on the Windy website. <https://www.windy.com/ru> (accessed on 20 February 2022). A graphical and numerical representation of air mass transport trajectories is available using the NOAA Air Resources Laboratory Internet resource. www.arl.noaa.gov (accessed on 11 February 2022). The concentration fields of dust, black carbon and other characteristics of atmospheric pollutants obtained from MERRA-2 reanalysis are available on the Internet resource <https://giovanni.gsfc.nasa.gov/giovanni/> (accessed on 15 February 2022). Fire maps are available on the Internet resource: SCANEX Fire Map. Available online: <https://fires.ru/> (accessed on 3 November 2021).

Acknowledgments: The authors thank V. A. Lebedev, Y. V. Zhulanov, Y. I. Obvintsev, A. A. Khapaev, L. O. Maksimenkov for help in organizing and carrying out field observations of near-surface aerosol parameters in Moscow and Kalmykia.

Conflicts of Interest: The authors declare no conflict of interest. The funders had no role in the design of the study; in the collection, analyses, or interpretation of data; in the writing of the manuscript, or in the decision to publish the results.

References

1. Sokhi, R.S.; Singh, V.; Querol, X.; Finardi, S.; Targino, A.C.; de Fatima Andrade, M.; Zavala, M. A global observational analysis to understand changes in air quality during exceptionally low anthropogenic emission conditions. *Environ. Intern.* **2021**, *157*, 106818. [[CrossRef](#)] [[PubMed](#)]
2. Seinfeld, J.; Pandis, S. *Atmospheric Chemistry and Physics: From Air Pollution to Climate Change*, 2nd ed.; John Wiley & Sons, Inc.: New York, NY, USA, 2006; p. 1248.
3. *AMAP Assessment 2015: Black Carbon and Ozone as Arctic Climate Forcers*; Arctic Monitoring and Assessment Programme (AMAP): Oslo, Norway, 2015; 116p, ISBN 9788279710929.
4. IPCC. Climate Change 2014: Synthesis Report. In *Contribution of Working Groups I, II and III to the Fifth Assessment Report of the Intergovernmental Panel on Climate Change*; Core Writing Team, Pachauri, R.K., Meyer, L.A., Eds.; IPCC: Geneva, Switzerland, 2014; 151p.
5. Cess, R.; Potter, G.; Ghan, S.; Gates, W.L. The climatic effects of large injections of atmospheric smoke and dust: A study of climate feedback mechanisms with one- and three-dimensional climate models. *J. Geophysical. Res.* **1980**, *90*, 12937–12950. [[CrossRef](#)]
6. Crutzen, P.J.; Andreae, M.O. Biomass Burning in the Tropics: Impact on Atmospheric Chemistry and Biogeochemical Cycles. *Science* **1990**, *250*, 1669–1678. [[CrossRef](#)]
7. Langmann, B.; Duncan, B.; Textor, C.; Trentmann, J.; van der Werf, G.R. Vegetation fire emissions and their impact on air pollution and climate. *Atmos. Environ.* **2009**, *43*, 107–116. [[CrossRef](#)]
8. Reid, J.; Koppmann, R. A review of biomass burning emissions part II: Intensive physical properties of biomass burning particles. *Atmos. Chem. Phys.* **2005**, *5*, 799–825. [[CrossRef](#)]
9. Schepanski, K. Transport of mineral dust and its impact on climate. *Geosciences* **2018**, *8*, 151. [[CrossRef](#)]
10. Chaibou, S.; Ma, A.; Sha, T. Dust radiative forcing and its impact on surface energy budget over West Africa. *Sci. Rep.* **2020**, *10*, 12236. [[CrossRef](#)] [[PubMed](#)]
11. Budyko, M.; Golitsyn, G.; Izrael, Y. *Global Climatic Catastrophes*; Springer: New York, NY, USA, 1988.
12. Xiong, J.; Zhao, T.; Bai, Y.; Liu, Y.; Han, Y.; Guo, C. Climate characteristics of dust aerosol and its transport in major global dust source regions. *J. Atmos. Sol.-Terr. Phys.* **2020**, *209*, 105415. [[CrossRef](#)]
13. Targino, A.C.; Krecl, P.; Johansson, C.; Swietlicki, E.; Massling, A.; Coraiola, G.C.; Lihavainen, H. Deterioration of air quality across Sweden due to transboundary agricultural burning emissions. *Boreal. Environ. Res.* **2013**, *18*, 19–36.
14. Bergin, M.S.; West, J.J.J.; Keating, T.J.; Russell, A.G. Regional Atmospheric Pollution and Transboundary Air Quality Management. *Annu. Rev. Environ. Resour.* **2005**, *30*, 1–37. [[CrossRef](#)]
15. Heilman, W.E.; Liu, Y.; Urbanski, S.; Kovalev, V.; Mickler, R. Wildland fire emissions, carbon, and climate: Plume rise, atmospheric transport, and chemistry processes. *For. Ecol. Manag.* **2014**, *317*, 70–79. [[CrossRef](#)]
16. Hernandez, A.J.; Morales-Rincon, L.A.; Wu, D.; Mallia, D.; Lin, J.C.; Jimenez, R. Transboundary transport of biomass burning aerosols and photochemical pollution in the Orinoco River Basin. *Atmos. Environ.* **2019**, *205*, 1–8. [[CrossRef](#)]
17. Gorchakov, G.I.; Kopeikin, V.M.; Sitnov, S.A.; Semoutnikova, E.G.; Sviridenkov, M.A.; Karpov, A.V.; Lezina, E.A.; Emilenko, A.S.; Isakov, A.A.; Kuznetsov, G.A.; et al. Moscow smoke haze in October 2014. Variations in the aerosol mass concentration. *Atmos. Ocean. Opt.* **2016**, *29*, 5–11. [[CrossRef](#)]

18. Gorchakov, G.I.; Karpov, A.V.; Kuznetsov, G.A.; Semoutnikova, E.G. Moscow smoke haze in October 2014: Variations in gaseous air pollutants. *Atmos. Ocean. Opt.* **2017**, *30*, 542–549. [[CrossRef](#)]
19. Popovicheva, O.; Kireeva, E.; Persiantseva, N.; Timofeev, M.; Kistler, M.; Kasper-Giebl, A.; Kopeikin, V. Physicochemical characterization of smoke aerosol during large-scale wildfires: Extreme event of August 2010 in Moscow. *Atmos. Environ.* **2014**, *96*, 405–414. [[CrossRef](#)]
20. Popovicheva, O.B.; Kireeva, E.D.; Persiantseva, N.M.; Timofeev, M.A.; Kistler, M.; Shoniya, N.K.; Kopeikin, V.M. Aerosol composition and microstructure in the smoky atmosphere of Moscow during the August 2010 extreme wildfires. *Izv. Atmos. Ocean. Phys.* **2017**, *53*, 49–57. [[CrossRef](#)]
21. Kopeikin, V.M.; Golitsyn, G.S.; Gengchen, W.; Pucal, W.; Ponomareva, T.Y. Variations in soot concentrations in megacities of Beijing and Moscow. *Atmos. Ocean. Opt.* **2019**, *32*, 540–544. [[CrossRef](#)]
22. Kopeikin, V.M.; Emilenko, A.S.; Isakov, A.A.; Loskutova, O.V.; Ponomareva, T.Y. Variability of soot and fine aerosol in the Moscow region in 2014–2016. *Atmos. Ocean. Opt.* **2018**, *31*, 243–249. [[CrossRef](#)]
23. Sitnov, S.A.; Gorchakov, G.I.; Sviridenkov, M.A.; Karpov, A.V. Evolution and radiation effects of the extreme smoke pollution over the European part of Russia in the summer of 2010. *Dokl. Earth Sci.* **2012**, *446*, 1197–1203. [[CrossRef](#)]
24. Popovicheva, O.; Padoan, S.; Schnelle-Kreis, J.; Nguyen, D.L.; Adam, T.; Kistler, M.; Steinkogler, T.; Kasper-Giebl, A.; Zimmermann, R.; Chubarova, N. Spring Aerosol in Urban Atmosphere of Megacity: Analytical and Statistical Assessment for Source Impacts. *Aerosol. Air Qual. Res.* **2020**, *20*, 702–719. [[CrossRef](#)]
25. Trefilova, A.V.; Artamonova, M.S.; Kuderina, T.M.; Gubanova, D.P.; Davydov, K.A.; Iordanskii, M.A.; Grechko, E.I.; Minashkin, V.M. Chemical composition and microphysical characteristics of atmospheric aerosol over Moscow and its vicinity in June 2009 and during the fire peak of 2010. *Izv. Atmos. Ocean. Phys.* **2013**, *49*, 765–778. [[CrossRef](#)]
26. Gubanova, D.P.; Vinogradova, A.A.; Iordanskii, M.A.; Skorokhod, A.I. Time Variations in the Composition of Atmospheric Aerosol in Moscow in Spring 2020. *Izv. Atmos. Ocean. Phys.* **2021**, *57*, 297–309. [[CrossRef](#)]
27. Kuznetsova, I.N. The effect of meteorology on air pollution in Moscow during the Summer episodes of 2010. *Izv. Atmos. Ocean. Phys.* **2012**, *48*, 504–515. [[CrossRef](#)]
28. Gorchakova, I.A.; Mokhov, I.I.; Rublev, A.N. Radiation and temperature effects of the intensive injection of dust aerosol into the atmosphere. *Izv. Atmos. Ocean. Phys.* **2015**, *51*, 113–126. [[CrossRef](#)]
29. Gorchakov, G.I.; Sitnov, S.A.; Karpov, A.V.; Gorchakova, I.A.; Gushchin, R.A.; Datsenko, O.I. Large-scale hazes over Eurasia in July 2016: Siberian smoke haze evolution. *IOP Conf. Ser. Earth Environ. Sci.* **2019**, *231*, 012019. [[CrossRef](#)]
30. Gorchakov, G.I.; Sitnov, S.A.; Semoutnikova, E.G.; Kopeikin, V.M.; Karpov, A.V.; Gorchakova, I.A.; Pankratova, N.V.; Ponomareva, T.Y.; Kuznetsov, G.A.; Loskutova, O.V.; et al. Large-scale smoke haze over the European part of Russia and Belarus in July 2016. *Izv. Atmos. Ocean. Phys.* **2018**, *54*, 986–996. [[CrossRef](#)]
31. ChooChuay, C.; Pongpiachan, S.; Tipmanee, D.; Deelman, W.; Suttinun, O.; Wang, Q.; Xing, L.; Li, G.; Han, Y.; Palakun, J.; et al. Long-range Transboundary Atmospheric Transport of Polycyclic Aromatic Hydrocarbons, Carbonaceous Compositions, and Water-soluble Ionic Species in Southern Thailand. *Aerosol. Air Qual. Res.* **2020**, *20*, 1591–1606. [[CrossRef](#)]
32. Hodshire, A.L.; Akherati, A.; Alvarado, M.J.; Brown-Steiner, B.; Jathar, S.H.; Jimenez, J.L.; Kreidenweis, S.M.; Lonsdale, C.R.; Onasch, T.B.; Ortega, A.M.; et al. Aging Effects on Biomass Burning Aerosol Mass and Composition: A Critical Review of Field and Laboratory Studies. *Environ. Sci. Technol.* **2019**, *53*, 10007–10022. [[CrossRef](#)] [[PubMed](#)]
33. Shimada, K.; Takami, A.; Ishida, T.; Taniguchi, Y.; Hasegawa, S.; Chan, C.K.; Kim, Y.P.; Lin, N.H.; Hatakeyama, S. Long-term Measurements of Carbonaceous Aerosol at Cape Hedo, Okinawa, Japan: Effects of Changes in Emissions in East Asia. *Aerosol. Air Qual. Res.* **2021**, *21*, 200505. [[CrossRef](#)]
34. Das, S.; Colarco, P.R.; Oman, L.D.; Taha, G.; Torres, O. The long-term transport and radiative impacts of the 2017 British Columbia pyrocumulonimbus smoke aerosols in the stratosphere. *Atmos. Chem. Phys.* **2021**, *21*, 12069–12090. [[CrossRef](#)]
35. Duc, H.N.; Chang, L.T.-C.; Azzi, M.; Jiang, N. Smoke aerosols dispersion and transport from the 2013 New South Wales (Australia) bushfires. *Environ. Monit. Assess* **2018**, *190*, 428. [[CrossRef](#)]
36. Noda, J.; Bergström, R.; Kong, X.; Gustafsson, T.L.; Kovacevik, B.; Svane, M.; Pettersson, J.B.C. Aerosol from Biomass Combustion in Northern Europe: Influence of Meteorological Conditions and Air Mass History. *Atmosphere* **2019**, *10*, 789. [[CrossRef](#)]
37. Martins, L.D.; Hallak, R.; Alves, R.C.; de Almeida, D.S.; Squizzato, R.; Moreira, C.A.; Beal, A.; da Silva, I.; Rudke, A.; Martins, J.A. Long-range Transport of Aerosols from Biomass Burning over Southeastern South America and their Implications on Air Quality. *Aerosol. Air Qual. Res.* **2018**, *18*, 1734–1745. [[CrossRef](#)]
38. Pereira, G.; Shimabukuro, Y.E.; Moraes, E.C.; Freitas, S.R.; Cardozo, F.S.; Longo, K.M. Monitoring the transport of biomass burning emission in South America. *Atmos. Pollut. Res.* **2011**, *2*, 247–254. [[CrossRef](#)]
39. Ulke, A.G. Influence of Regional Transport Mechanisms on the Fingerprint of Biomass-Burning Aerosols in Buenos Aires. *Hindawi Adv. Meteorol.* **2019**, *2019*, 6792161. [[CrossRef](#)]
40. Duc, H.N.; Bang, H.Q.; Quang, N.X. Modelling and prediction of air pollutant transport during the 2014 biomass burning and forest fires in peninsular Southeast Asia. *Environ Monit. Assess* **2016**, *188*, 106. [[CrossRef](#)]
41. Marelle, L.; Raut, J.-C.; Thomas, J.L.; Law, K.S.; Quennehen, B.; Ancellet, G.; Pelon, J.; Schwarzenboeck, A.; Fast, J.D. Transport of anthropogenic and biomass burning aerosols from Europe to the Arctic during spring 2008. *Atmos. Chem. Phys.* **2015**, *15*, 3831–3850. [[CrossRef](#)]

42. Ancellet, G.; Pelon, J.; Totems, J.; Chazette, P.; Bazureau, A.; Sicard, M.; Di Iorio, T.; Dulac, F.; Mallet, M. Long-range transport and mixing of aerosol sources during the 2013 North American biomass burning episode: Analysis of multiple lidar observations in the western Mediterranean basin. *Atmos. Chem. Phys.* **2016**, *16*, 4725–4742. [[CrossRef](#)]
43. Das, S.; Harshvardhan, H.; Huisheng, B.; Chin, M.; Curci, G.; Protonotariou, A.P.; Mielonen, T.; Zhang, K.; Wang, H.; Liu, X. Biomass burning aerosol transport and vertical distribution over the South African-Atlantic region. *JGR Atmos.* **2017**, *122*, 6391–6415. [[CrossRef](#)]
44. Ginoux, P.; Prospero, J.M.; Gill, T.E.; Hsu, N.C.; Zhao, M. Global-scale attribution of anthropogenic and natural dust sources and their emission rates based on MODIS Deep Blue aerosol products. *Rev. Geophysics.* **2012**, *50*, RG3005. [[CrossRef](#)]
45. Prospero, J. Long-range transport of mineral dust in the global atmosphere: Impact of African dust on the environment of the southeastern United States. *Proc. Natl. Acad. Sci. USA* **1999**, *96*, 3396–3403. [[CrossRef](#)]
46. Guedes, A.G.; Landulfo, E.; Montilla-Rosero, E.; Lopes, F.J.; Hoelzemann, J.J.; Fernandez, J.H.; Silva, M.P.A.; Santos, R.S.S.; Guerrero-Rascado, J.L.; Alados-Arboledas, L. Detection of Saharan mineral dust aerosol transport over Brazilian northeast through a depolarization lidar. *EPJ Web Conf.* **2018**, *176*, 05036. [[CrossRef](#)]
47. Weinzierl, B.; Ansmann, A.; Prospero, J.M.; Althausen, D.; Benker, N.; Chouza, F.; Dollner, M.; Farrell, D.; Fomba, W.K.; Freudenthaler, V.; et al. The Saharan Aerosol Long-Range Transport and Aerosol-Cloud-Interaction Experiment: Overview and Selected Highlights. *Bull. Am. Meteorol. Soc.* **2017**, *98*, 1427–1451. [[CrossRef](#)]
48. van der Does, M.; Knippertz, P.; Zschenderlein, P.; Harrison, R.G.; Stuut, J.-B.W. The mysterious long-range transport of giant mineral dust particles. *Sci. Adv.* **2018**, *4*, eaau2768. [[CrossRef](#)] [[PubMed](#)]
49. Asher, E.C.; Christensen, J.N.; Post, A.; Perry, K.; Cliff, S.S.; Zhao, Y.; Trousdell, J.; Faloon, I. The transport of Asian dust and combustion aerosols and associated ozone to North America as observed from a mountain top monitoring site in the California coast range. *JGR Atmos.* **2018**, *123*, 4890–4909. [[CrossRef](#)]
50. Yu, H.; Chin, M.; Bian, H.; Yuan, T.; Prospero, J.; Omar, A.H.; Remer, L.A.; Winker, D.M.; Yang, Y.; Zhang, Y.; et al. Quantification of trans-Atlantic dust transport from seven-year (2007–2013) record of CALIPSO lidar measurements. *Remote Sens. Environ.* **2015**, *159*, 232–249. [[CrossRef](#)]
51. Conceição, R.; Silva, H.G.; Mirao, J.; Gostein, M.; Fialho, L.; Narvarte, L.; Collares-Pereira, M. Saharan dust transport to Europe and its impact on photovoltaic performance: A case study of soiling in Portugal. *Sol. Energy* **2018**, *160*, 94–102. [[CrossRef](#)]
52. Israelevich, P.L.; Ganor, E.; Alpert, P.; Kishcha, P.; Stupp, A. Predominant transport paths of Saharan dust over the Mediterranean Sea to Europe. *JGR Atmos.* **2012**, *117*, 2205. [[CrossRef](#)]
53. Palacios-Peña, L.; Lorente-Plazas, R.; Montávez, J.P.; Jiménez-Guerrero, P. Saharan Dust Modeling Over the Mediterranean Basin and Central Europe: Does the Resolution Matter? *Front. Earth Sci.* **2019**, *7*, 290. [[CrossRef](#)]
54. Salvador, P.; Artinano, B.; Molero, F.; Viana, M.; Pey, J.; Alastuey, A.; Querol, X. African dust contribution to ambient aerosol levels across central Spain: Characterization of long-range transport episodes of desert dust. *Atmos. Res.* **2013**, *127*, 117–129. [[CrossRef](#)]
55. Gkikas, A.; Basart, S.; Hatzianastassiou, N.; Marinou, E.; Amiridis, V.; Kazadzis, S.; Pey, J.; Querol, X.; Jorba, O.; Gassó, S.; et al. Mediterranean intense desert dust outbreaks and their vertical structure based on remote sensing data. *Atmos. Chem. Phys.* **2016**, *16*, 8609–8642. [[CrossRef](#)]
56. Meloni, D.; di Sarra, A.; Biavati, G.; DeLuisi, J.; Monteleone, F.; Pace, G.; Piacentino, S.; Sferlazzo, D. Seasonal behavior of Saharan dust events at the Mediterranean island of Lampedusa in the period 1999–2005. *Atmos. Environ.* **2007**, *41*, 3041–3056. [[CrossRef](#)]
57. Guerzoni, S.; Molinaroli, E.; Chester, R. Saharan dust inputs to the western Mediterranean Sea: Depositional patterns, geochemistry and sedimentological implications. *Deep Sea Res.* **1997**, *44*, 631–654. [[CrossRef](#)]
58. Hu, Z.; Huang, J.; Zhao, C.; Jin, Q.; Ma, Y.; Yang, B. Modeling dust sources, transport, and radiative effects at different altitudes over the Tibetan Plateau. *Atmos. Chem. Phys.* **2020**, *20*, 1507–1529. [[CrossRef](#)]
59. Huang, J.; Minnis, P.; Chen, B.; Huang, Z.; Liu, Z.; Zhao, Q.; Yi, Y.; Ayers, J.K. Long-range transport and vertical structure of Asian dust from CALIPSO and surface measurements during PACDEX. *J. Geophys. Res.* **2008**, *113*, D23212. [[CrossRef](#)]
60. Vijayakumar, K.; Devara, P.; Rao, S.V.B.; Jayasankar, C. Dust aerosol characterization and transport features based on combined ground-based, satellite and model-simulated data. *Aeolian Res.* **2016**, *21*, 75–85. [[CrossRef](#)]
61. Yang, L.; Shi, Z.; Sun, H.; Xie, X.; Liu, X.; An, Z. Distinct effects of winter monsoon and westerly circulation on dust aerosol transport over East Asia. *Theor. Appl. Climatol.* **2021**, *144*, 1031–1042. [[CrossRef](#)]
62. Kondratyev, I.; Kachur, A.; Yurchenko, S.; Mezentseva, L.I.; Roschupkin, G.T.; Semykina, G.I. Synoptic and geochemical aspects of abnormal dust transfer in south Primorskii krai. *Vestn. Far East Branch Russ. Acad. Sci.* **2005**, *3*, 55–65. (In Russian)
63. Abdullaev, S.F.; Maslov, V.A.; Nazarov, B.I.; Madvaliev, U.; Davlatshoev, T. The elemental composition of soils and dust aerosol in the south-central part of Tajikistan. *Atmos. Ocean. Opt.* **2015**, *28*, 347–358. [[CrossRef](#)]
64. Huang, Z.; Huang, J.; Hayasaka, T.; Wang, S.; Zhou, T.; Jin, H. Short-cut transport path for Asian dust directly to the Arctic: A case study. *Environ. Res. Lett.* **2015**, *10*, 114018. [[CrossRef](#)]
65. Gubanova, D.P.; Vinogradova, A.A.; Skorokhod, A.A.; Iordanskii, M.A. Abnormal aerosol air pollution in Moscow near the local anthropogenic source in July 2021. *Hydrometeorol. Res. Forecast.* **2021**, *4*, 133–147. Available online: <http://method.meteorf.ru/publ/tr/tr382/htm/08.htm> (accessed on 27 February 2022). (In Russian) [[CrossRef](#)]
66. Shukurov, K.; Shukurova, L. Aral's potential sources of dust for Moscow region. *E3S Web Conf.* **2019**, *99*, 02015. [[CrossRef](#)]
67. Shukurov, K.; Shukurova, L. Source regions of ammonium nitrate, ammonium sulfate, and natural silicates in the surface aerosols of Moscow oblast. *Izv. Atmos. Ocean. Phys.* **2017**, *53*, 316–325. [[CrossRef](#)]

68. Shukurov, K.; Chkhetiani, O. Probability of transport of air parcels from the arid lands in the Southern Russia to Moscow region. *Proc. SPIE* **2017**, *10466*, 104663V. [CrossRef]
69. Lokoshchenko, M.A.; Elansky, N.F.; Trifanova, A.V.; Belikov, I.B.; Skorokhod, A.I. About extreme levels of air pollution in Moscow. *Vestn. Mosk. Universiteta. Seriya 5 Geogr.* **2016**, *4*, 29–39. (In Russian)
70. Air Pollution in Moscow. Available online: <https://sud-expertiza.ru/zagryaznenie-vozduha-v-moskve/> (accessed on 27 February 2022).
71. Mosecomonitoring. Air Quality in Moscow. Available online: <https://mosecom.mos.ru/air-quality/> (accessed on 27 February 2022).
72. Kulbachevsky, A.O. Report “On the State of the Environment in the City of Moscow in 2010; NIPI IGSP: Moscow, Russia, 2011; 135p. Available online: <https://mosecom.mos.ru/wp-content/uploads/2018/02/report2010.pdf> (accessed on 27 February 2022). (In Russian)
73. AFA Filters. Available online: https://eng.fgsiz.ru/product/product/index/product_id/143/?path=75 (accessed on 27 February 2022).
74. Karandashev, V.K.; Turanov, A.N.; Orlova, T.A.; Lezhnev, A.E.; Nosenko, S.V.; Zolotareva, N.I.; Moskvina, I.R. Use of mass spectrometry with inductively coupled plasma method for element analysis of surrounding medium objects. *Ind. Laboratory. Diagn. Mater.* **2007**, *73*, 12–22. (In Russian)
75. Kudryashov, V.I. Analysis of the elemental composition atmospheric aerosols by physical methods. In *Problemy Fiziki Atmosfery: Mezhdvuzovskii Sbornik (Problems of Atmospheric Physics: Interuniversity Transactions)*; SPbGU Publ.: Saint-Petersburg, Russia, 1997; pp. 97–130. (In Russian)
76. Erhardt, H. *Rentgenofluorescentnyj Analiz. Primenenie v Zavodskih Laboratorijah*; Metallurgija Publ.: Moscow, Russia, 1985; 254p. (In Russian)
77. Windy. Available online: <https://www.windy.com/ru> (accessed on 20 February 2022).
78. Reliable Prognosis. Available online: <https://rp5.ru> (accessed on 16 December 2021).
79. Weatherarchive. Available online: <http://weatherarchive.ru/Pogoda/Moscow> (accessed on 12 January 2022).
80. Stein, A.F.; Draxler, R.R.; Rolph, G.D.; Stunder, B.J.B.; Cohen, M.D.; Ngan, F. NOAA’s HYSPLIT atmospheric transport and dispersion modeling system. *Bull. Amer. Meteor. Soc.* **2015**, *96*, 2059–2077. [CrossRef]
81. Rolph, G.; Stein, A.; Stunder, B. Real-time Environmental Applications and Display sYstem: READY. *Environ. Model. Softw.* **2017**, *95*, 210–228. [CrossRef]
82. NOAA Air Resources Laboratory. Available online: www.arl.noaa.gov (accessed on 11 February 2022).
83. SCANEX Fire Map. Available online: <https://fires.ru/> (accessed on 3 November 2021).
84. NASA Fire Information for Resource Management System (FIRMS). Available online: <https://firms.modaps.eosdis.nasa.gov> (accessed on 11 November 2021).
85. MERRA-2. Available online: <https://giovanni.gsfc.nasa.gov/giovanni/> (accessed on 15 February 2022).
86. Mosecomonitoring. Available online: <https://mosecom.mos.ru> (accessed on 17 February 2022).
87. Gubanova, D.P.; Elansky, N.F.; I Skorokhod, A.; Kuderina, T.M.; A Iordansky, M.; Sadovskaya, N.V.; Anikin, P.P. Physical and chemical properties of atmospheric aerosols in Moscow and its suburb for climate assessments. *IOP Conf. Ser. Earth Environ. Sci.* **2020**, *606*, 012019. [CrossRef]
88. Gubanova, D.P.; Iordanskii, M.A.; Kuderina, T.M.; Skorokhod, A.I.; Elansky, N.F.; Minashkin, V.M. Elemental Composition of Aerosols in the Ground Air of Moscow: Seasonal Changes in 2019 and 2020. *Atmos. Ocean. Opt.* **2021**, *34*, 475–482. [CrossRef]
89. World Health Organization. *Occupational and Environmental Health Team. WHO Air Quality Guidelines for Particulate Matter, Ozone, Nitrogen Dioxide and Sulfur Dioxide: Global Update 2005: Summary of Risk Assessment*; World Health Organization: Geneva, Switzerland, 2006. Available online: <https://apps.who.int/iris/handle/10665/69477> (accessed on 27 February 2022).
90. Vinogradova, A.A.; Gubanova, D.P.; Iordanskii, M.A.; Skorokhod, A.I. The influence of meteorological conditions and long-range air mass transport on the composition of near-surface aerosol in Moscow during the winter seasons. *Atmos. Ocean. Opt.* **2022**, submitted.
91. Kuznetsova, I.N.; Glazkova, A.A.; Shalygina, I.Y.; Nakhaev, M.I.; Arkhangel’skaya, A.A.; Zvyagintsev, A.M.; Semutnikova, E.G.; Zakharova, P.V.; Lezina, E.A. Seasonal and diurnal variability of particulate matter PM₁₀ in surface air of Moscow habitable districts. *Atmos. Ocean. Opt.* **2014**, *6*, 473–482.
92. Gubanova, D.P.; Belikov, I.B.; Elansky, N.F.; Skorokhod, A.I.; Chubarova, N.E. Variations in PM_{2.5} surface concentration in Moscow according to observations at MSU meteorological observatory. *Atmos. Ocean. Opt.* **2018**, *31*, 290–299. [CrossRef]
93. Ivlev, L.S. *Khimicheskii Sostav i Struktura Atmosferynykh Aerozolei (Chemical Composition and Structure of Atmospheric Aerosols)*; Leningrad State University: Leningrad, Russia, 1982. (In Russian)
94. Chkhetiani, O.G.; Vazaeva, N.V.; Chernokulsky, A.V.; Shukurov, K.A.; Gubanova, D.P.; Artamonova, M.S.; Maksimenkov, L.O.; Kozlov, F.A.; Kuderina, T.M. Analysis of Mineral Aerosol in the Surface Layer over the Caspian Lowland Desert by the Data of 12 Summer Field Campaigns in 2002–2020. *Atmosphere* **2021**, *12*, 985. [CrossRef]
95. Vinogradova, A.A.; Malkov, I.P.; Polissar, A.V.; Khranov, N.N. Elemental composition of surface atmospheric aerosol in the Russian Arctic region. *Izv. Akad. Nauk Fiz. Atmos. Okeana.* **1993**, *29*, 164–172.
96. Bortnikov, V.Y.; Bukatyi, V.I.; Ryabinin, I.V.; Semenov, G.A. Microphysical parameters and elemental composition of atmospheric aerosol in the town of Barnaul in 2006–2008. *Izv. Altai. Gos. Univ.* **2009**, *61*, 106–110. (In Russian)

97. Lukashin, V.N.; Novigatsky, A.N. Chemical composition of aerosols in the near-water surface atmospheric layer of the Central Caspian Sea in the winter and autumn of 2005. *Oceanology* **2013**, *53*, 727–738. [[CrossRef](#)]
98. Smolík, J.; Ždímal, V.; Schwarz, J.; Lazaridis, M.; Havárnek, V.; Eleftheriadis, K.; Mihalopoulos, N.; Bryant, C.; Colbeck, I. Size resolved mass concentration and elemental composition of atmospheric aerosols over the Eastern Mediterranean area. *Atmos. Chem. Phys.* **2003**, *3*, 2207–2216. [[CrossRef](#)]
99. Bergbäck, B.; Johansson, K.; Mohlander, U. Urban metal flows—A case study of Stockholm. Review and Conclusions. *Water Air Soil Pollut. Focus* **2001**, *1*, 3–24. [[CrossRef](#)]
100. Samek, L.; Turek-Fijak, A.; Skiba, A.; Furman, P.; Styszko, K.; Furman, L.; Stegowski, Z. Complex Characterization of Fine Fraction and Source Contribution to PM_{2.5} Mass at an Urban Area in Central Europe. *Atmosphere* **2020**, *11*, 1085. [[CrossRef](#)]
101. Varrica, D.; Dongarrà, G.; Sabatino, G.; Monna, F. Inorganic geochemistry of roadway dust from the metropolitan area of Palermo, Italy. *Environ. Geol.* **2003**, *44*, 222–230. [[CrossRef](#)]
102. Theodosi, C.; Tsagkaraki, M.; Zampas, P.; Grivas, G.; Liakakou, E.; Paraskevopoulou, D.; Lianou, M.; Gerasopoulos, E.; Mihalopoulos, N. Multi-year chemical composition of the fine-aerosol fraction in Athens, Greece, with emphasis on the contribution of residential heating in wintertime. *Atmos. Chem. Phys.* **2018**, *18*, 14371–14391. [[CrossRef](#)]
103. Gebre, G.; Feleke, Z.; Sahle-Demissie, E. Mass concentrations and elemental composition of urban atmospheric aerosols in Addis Ababa, Ethiopia. *Bull. Chem. Soc. Ethiop.* **2010**, *24*, 361–373. [[CrossRef](#)]
104. Offor, I.F.; Adie, G.U.; Ana, G.R. Review of Particulate Matter and Elemental Composition of Aerosols at Selected Locations in Nigeria from 1985–2015. *J. Health Pollut.* **2016**, *10*, 1–18. [[CrossRef](#)] [[PubMed](#)]
105. Klopper, D.; Formenti, P.; Namwoonde, A.; Cazaunau, M.; Chevaillier, S.; Feron, A.; Gaimoz, C.; Hease, P.; Lahmidi, F.; Mirandebret, C.; et al. Chemical composition and source apportionment of atmospheric aerosols on the Namibian coast. *Atmos. Chem. Phys.* **2020**, *20*, 15811–15833. [[CrossRef](#)]
106. Kulshrestha, A.; Gursumeeran, P.S.; Masiha, J.; Taneja, A. Metal concentration of PM_{2.5} and PM₁₀ particles and seasonal variations in urban and rural environment of Agra, India. *Sci. Total Environ.* **2009**, *407*, 6196–6204. [[CrossRef](#)] [[PubMed](#)]
107. Atar Singh Pipal, A.S.; Jan, R.; Satsangi, P.G.; Tiwari, S.; Taneja, A. Study of Surface Morphology, Elemental Composition and Origin of Atmospheric Aerosols (PM_{2.5} and PM₁₀) over Agra, India. *Aerosol Air Qual. Res.* **2014**, *14*, 1685–1700. [[CrossRef](#)]
108. Zhang, R.; Han, Z.; Shen, Z.; Cao, J. Continuous measurement of number concentrations and elemental composition of aerosol particles for a dust storm event in Beijing. *Adv. Atmos. Sci.* **2008**, *25*, 89–95. [[CrossRef](#)]
109. Volokh, A.A.; Zhuravleva, M.G. Assessment of anthropogenic air pollution in Moscow. *Izv. Akad. Nauk Fiz. Atmos. Okeana.* **1994**, *30*, 182–188.
110. Ogorodnikov, B.I.; Budyka, A.K.; Skitovich, V.I.; Brodovoi, A.V. Characteristics of aerosols in the boundary layer of the atmosphere over Moscow. *Izv. Atmos. Ocean. Phys.* **1996**, *32*, 149–157.
111. Pacyna, J.M. Source inventories for atmospheric trace metals. In *Atmospheric Particles*; Harrison, R.M., Van Grieken, R., Eds.; Wiley: Chichester, UK, 1998; pp. 385–423.
112. Milford, J.B.; Davidson, C.I. The sizes of particulate trace elements in the atmosphere—A review. *J. Air Pollut. Control. Assoc.* **1985**, *35*, 1249–1260. [[CrossRef](#)] [[PubMed](#)]
113. Ivanov, V.V. Ecological Geochemistry of Elements. In *Major P-Elements*; Nedra: Moscow, Russia, 1994; 303p. (In Russian)
114. Perel'man, A.I.; Kasimov, N.S. *Landscape Geochemistry*; Astreya-2000: Moscow, Russia, 1999; 610p. (In Russian)
115. Kasimov, N.S. *Landscape Ecogeochemistry*; Filimonov, M.V.: Moscow, Russia, 2013; 208p. (In Russian)
116. Dobrovol'skii, V.V. *Biogeokhimiya Mirovoi Sushy (Biogeochemistry of World Land)*; Nauch. Mir: Moscow, Russia, 2009; 440p. (In Russian)
117. SanPiN 1.2.3685-21. Hygienic Standards and Requirements for Ensuring Safety and (or) Harmlessness to Humans from Environmental Factors. Available online: <https://tk-expert.ru/uploads/files/ntd/ntd-861-20210304-191207.pdf> (accessed on 27 February 2022). (In Russian)